UNIVERSITY OF CALIFORNIA, SAN DIEGO

Developing a Pervasive Brain-Computer Interface System for Naturalistic Brain Dynamics

A dissertation submitted in partial satisfaction of the requirements for the degree Doctor of Philosophy

in

Computer Science (Computer Engineering)

by

Yu-Te Wang

Committee in charge:

Professor Chung-Kuan Cheng, Chair
Professor Tzyy-Ping Jung, Co-Chair
Professor Gert Cauwenberghs
Professor Ryan Kastner
Professor Scott Klemmer

2015

The Dissertation of Yu-Te Wang is approved and is acceptable in quality and form for publication on microfilm and electronically:

_____

_____

_____

_____

Co-Chair

_____

Chair

University of California, San Diego

2015

EPIGRAPH

Love your life, perfect your life, beautify all things in your life.
Prepare a noble death song for the day when you go over the great divide.
When it comes your time to die,
be not like those whose hearts are filled with the fear of death,
so that when their time comes they weep and pray for a little more time to live their lives over again in a different way.
Sing your death song and die like a hero going home.

Chief Tecumseh (Poem from Act of Valor)

TABLE OF CONTENTS

LIST OF FIGURES

LIST OF TABLES

Acknowledgements

I will always remember my first experience using the computer in junior high. It was equipped with a cutting-edge Pentium II processor, and running the latest MS-DOS 6.2 OS. The task was just simply creating my homework schedule and printing it out, but I was fascinated. Although I was captivated by the moment, an inevitable question came rushing to my mind: Was it possible to control this instrument directly with my mind instead of through the limited means of a keyboard and mouse? Now, I am so glad and proud to say: I CAN MAKE IT!

I would like to acknowledge Professors Chung-Kuan Cheng and Tzyy-Ping Jung for their support as the chair/co-chair of my committee. Through my entire research and life in UCSD, their guidance has proved to be invaluable. Thanks to Professors Cauwenberghs Gert, Scott Klemmer, and Ryan Kastner for their valuable comments and feedback as my committee members. They provided many valuable suggestions for my research and improved the quality of the dissertation.

I especially want to thank Yijun Wang. His brilliant mind encouraged and helped me to overcome the numerous difficulties in the research. I would also like to thank my collaborators at Swartz Center for Computational Neuroscience. The teatime held in every afternoon always makes me relax and inspires me to action. I also want to thank all of my friends, the time we spent in every baseball game, spearfishing, pingpong, snowboarding, and so on really perfect and beautify my life.

Finally, I would like to acknowledge my lovely family. This journey would not have been possible without their support. This dissertation is dedicated to them.

Chapter 2, in part, contains materials from "Developing Stimulus Presentation on Mobile Devices for a truly Portable SSVEP-based BCI" by Yu-Te Wang, Yijun Wang, Chung-Kuan Cheng, and Tzyy-Ping Jung, which was published in the *IEEE Engineering in Medicine and Biology Society (IEEE EMBC 2013)*. The dissertation author was the first author of this paper.

Chapter 3, in part, contains materials from "Measuring Steady-State Visual Evoked Potentials from non-hair-bearing areas" by Yu-Te Wang, Yijun Wang, Chung-Kuan Cheng, and Tzyy-Ping Jung, which appeared in the *IEEE EMBC 2012*. The dissertation author was the first author of the paper.

Chapter 4, in part, contains materials from "A Smartphone Based Brain-Computer Interface for Communication in Daily Life" by Yu-Te Wang, Yijun Wang, and Tzyy-Ping Jung, which was published in the *Journal of Neural Engineering* Vol.8, No.2, 2011. The dissertation author was the first author of this paper.

Chapter 5, in part, contains materials from "Developing an EEG-based On-line Closed-loop Lapse Detection and Mitigation System" by Yu-Te Wang, Kuan-Chih Hunag, Chun-Shu Wei, Teng-Yi Huang, Li-Wei Ko, Chin-Teng Lin, Chung-Kuan Cheng, and Tzyy-Ping Jung, which was published in the *Frontiers in Neuroscience*, 2014. The dissertation author was the first author of this paper.

VITA

2005 **B.S.** in Computer Science, National Taiwan University of Science and Technology, Taiwan.

2009 **M.S.** in Biomedical Engineering, National Chiao Tung University, Taiwan.

2009 - 2011 Research assistant in Swartz Center for Computational Neuroscience.

2015 **Ph.D.** in Computer Science (Computer Engineering), University of California San Diego, La Jolla, U.S.A.

PUBLICATIONS

Journal Articles

- **Y.-T. Wang,** K. -C. Huang, C.-S. Wei, T.-Y. Huang, L.-W. Ko, C.-T. Lin, C.-K. Cheng, and T.-P. Jung, "Developing an EEG-based on-line closed-loop lapse detection and mitigation system", Frontiers Neuroscience, vol. 8, 2014.
- M. Nakanishi, Y. Wang, **Y.-T. Wang**, Y. Mitsukura and T. -P. Jung, "Generating Visual Flickers for Eliciting Robust Steady-State Visual Evoked Potentials at Flexible Frequencies Using Monitor Refresh Rate." PloS one, vol. 9, p. e99235, 2014.
- J. K. Zao, T.-T. Gan, C.-K. You, A.-T. Nguyen, **Y.-T. Wang**, C. Kothe, C. You, S. J. R. Méndez, N. Bigdely-Shamlo and C.-E. Chung, "Pervasive Brain Monitoring and Data Sharing with Multi-tiered Cloud Computing Infrastructure," Frontiers in Human Neuroscience, p. 0. 2014.
- M. Nakanish, Y. Wang, **Y.-T. Wang**, Y. Mitsukura and T.-P. Jung, "A High-Speed Brain Speller Using Steady-State Visual Evoked Potentials," International Journal of Neural Systems, 2014.
- Y. Wang, **Y.-T. Wang** and T.-P. Jung, "Translation of EEG Spatial filters from resting to motor imagery using independent component analysis," PloS one, vol. 7, p. e37665, 2012.
- **Y.-T. Wang**, Y. Wang and T.-P. Jung, "A smartphone-based brain–computer interface for communication in daily life," Journal of Neural Engineering, vol. 8, p. 025018, 2011.
- Y. Chi, **Y.-T. Wang**, C. Maier, T. Jung and G. Cauwenberghs, "Dry and Noncontact EEG Sensors for Mobile Brain Computer Interfaces," Neural Systems and Rehabilitation Engineering, IEEE Transactions on, pp. 1-1, 2011.
- Y. Wang, **Y.-T. Wang** and T.-P. Jung, "Visual stimulus design for high-rate SSVEP BCI," Electronics letters, vol. 46, pp. 1057-1058, 2010.

Conference Articles

- Y. Wang, M. Nakanishi, **Y.-T. Wang** and T.-P. Jung, "Enhancing detection of steady-state visual evoked potentials using individual training data," in Engineering in Medicine and Biology Society (EMBC), 36th Annual International Conference of the IEEE, 2014, pp. 3037-3040.
- M. Nakanishi, Y. Wang, **Y.-T. Wang**, Y. Mitsukura and T.-P. Jung, "Enhancing unsupervised canonical correlation analysis-based frequency detection of SSVEPs by incorporating background EEG," in Engineering in Medicine and Biology Society (EMBC), 36th Annual International Conference of the IEEE, 2014, pp. 3053-3056.
- C. -S. Wei, Y.-P. Lin, Y. Wang, **Y.-T. Wang** and T.-P. Jung, "Detection of steady-state visual-evoked potential using differential canonical correlation analysis," in Neural Engineering (NER), 6th International IEEE/EMBS Conference, 2013, pp. 57-60.
- **Y.-T. Wang**, Y. Wang, C.-K. Cheng and T.-P. Jung, "Developing stimulus presentation on mobile devices for a truly portable SSVEP-based BCI," in Engineering in Medicine and Biology Society (EMBC), 35th Annual International Conference of the IEEE, 2013, pp. 5271-5274.
- Y. Wang, N. Wong, **Y.-T. Wang**, Y. Wang, X. Huang, L. Huang, T.-P. Jung, A. J. Mandell and C.-K. Cheng, "Study of visual stimulus waveforms via forced van der Pol oscillator model for SSVEP-based brain-computer interfaces," in Communications, Circuits and Systems (ICCCAS), International Conference, 2013, pp. 475-479.
- M. Nakanishi, Y. Wang, **Y.-T. Wang**, Y. Mitsukura and T.-P. Jung, "Integrating interference frequency components elicited by monitor refresh rate to enhance frequency detection of SSVEPs," in Neural Engineering (NER), 6th International IEEE/EMBS Conference, 2013, pp. 1092-1095.
- M. Nakanishi, Y. Wang, **Y.-T. Wang**, Y. Mitsukura and T.-P. Jung, "An approximation approach for rendering visual flickers in SSVEP-based BCI using monitor refresh rate," in Engineering in Medicine and Biology Society (EMBC), 2013 35th Annual International Conference of the IEEE, 2013, pp. 2176-2179.
- L. Huang, X. Huang, **Y.-T. Wang**, Y. Wang, T.-P. Jung and C.-K. Cheng, "Empirical mode decomposition improves detection of SSVEP," in Engineering in Medicine and Biology Society (EMBC), 2013 35th Annual International Conference of the IEEE, 2013, pp. 3901-3904.
- **Y.-T. Wang**, C. Chen, K. Huang, C. Lin, Y. Wang and T. Jung, "Smartphone Based Drowsiness Monitoring and Management System," IEEE Biomedical Circuits and Systems Conference, pp. 200-203, 2012.
- **Y.-T. Wang**, Y. Wang, C.-K. Cheng and T.-P. Jung, "Measuring steady-state visual evoked potentials from non-hair-bearing areas," in Engineering in Medicine and Biology Society (EMBC), Annual International Conference of the IEEE, 2012, pp. 1806-1809.

- K. C. Tseng, **Y.-T. Wang**, B.-S. Lin and P. H. Hsieh, "Brain Computer Interface-based Multimedia Controller," in Intelligent Information Hiding and Multimedia Signal Processing (IIH-MSP), Eighth International Conference, 2012, pp. 277-280.
- C.-K. Chen, E. Chua, Z.-H. Hsieh, W.-C. Fang, **Y.-T. Wang** and T.-P. Jung, "An EEG-based brain—computer interface with real-time artifact removal using independent component analysis," in Consumer Electronics-Berlin (ICCE-Berlin), IEEE International Conference, 2012, pp. 13-14.
- Y. Wang, **Y.-T. Wang**, T.-P. Jung, X. Gao and S. Gao, "A collaborative brain-computer interface," in Biomedical Engineering and Informatics (BMEI), 4th International Conference, 2011, pp. 580-583.
- I.-J. Wang, L.-D. Liao, **Y.-T. Wang**, C.-Y. Chen, B.-S. Lin, S.-W. Lu and C.-T. Lin, "A Wearable Mobile Electrocardiogram measurement device with novel dry polymer-based electrodes," in TENCON 2010-2010 IEEE Region 10 Conference, 2010, pp. 379-384.

Book Chapters

- Y. M. Chi, Y. Wang, **Y.-T. Wang**, T.-P. Jung, T. Kerth and Y. Cao, "A practical mobile dry EEG system for human computer interfaces," in Foundations of Augmented Cognition, ed: Springer Berlin Heidelberg, 2013, pp. 649-655.
- C.-T. Lin, L.-W. Ko, C.-J. Chang, **Y.-T. Wang**, C.-H. Chung, F.-S. Yang, J.-R. Duann, T.-P. Jung and J.-C. Chiou, "Wearable and wireless brain-computer interface and its applications," in Foundations of augmented cognition. Neuroergonomics and operational neuroscience, ed: Springer Berlin Heidelberg, 2009, pp. 741-748.

ABSTRACT OF THE DISSERTATION

Developing a Pervasive Brain-Computer Interface System

for Naturalistic Brain Dynamics

by

Yu-Te Wang

Doctor of Philosophy in Computer Science (Computer Engineering)

University of California, San Diego, 2015

Professor Chung-Kuan Cheng, Chair
Professor Tzyy-ping Jung, Co-Chair

This work develops and tests two Brain-Computer Interface (BCI) systems. The first one is a Steady-state visual evoked potential (SSVEP)-based BCI system. This thesis explores every component of an SSVEP-based BCI system from the front-end to back-end, including the visual stimuli, electroencephalogram (EEG) data acquisition, signal processing and a modularized platform. This thesis also discusses how to move an SSVEP-based BCI system from a laboratory demonstration to a real-life application. Our neurological results show that: (1) it is feasible to precisely render visual stimuli on mobile devices; (2) the signal quality of the SSVEPs measured from

non-hair-bearing areas was comparable with, if not better than, that measured from hair-covered occipital areas; (3) it is practical to build a truly portable and wearable SSVEP-based BCI system integrating dry EEG sensors, miniature electronics, wireless telemetry, online signal-processing pipeline, and visual stimuli presentation on a smartphone. This work may significantly improve the practicality of an SSVEP-based BCI system for either real-life or clinical research.

The second one is an On-line Closed-loop Lapse Detection and Mitigation (OCLDM) System for detecting and mitigating driving fatigue. In this thesis we translate the above-mentioned BCI platform to develop and test an OCLDM System that mitigate transient fatigue during a sustained attention task in a simulated driving environment. This system features a mobile wireless dry-sensor EEG headgear and a smartphone-based real-time EEG processing platform. The on-line testing results of the OCLDM System demontrated the efficacy of the arousing signals in improving subjects' response times to the subsequent lane-departure events. This study may lead to a practical on-line lapse detection and mitigation system in real-world environments.

Chapter 1

Introduction

Brain-computer interface (BCI) systems acquire Electroencephalography (EEG) signals from the brain and translate them into digital commands that can be recognized and processed on computers using advanced algorithms [1]-[3]. More precisely, one can measure the voltage fluctuations from ionic current flows within the neurons of the brain as they are projected onto the scalp. This discovery opens the possibility of directly giving output commands from the brain to external devices and bypassing the traditional control path, i.e., from the central nervous system to the peripheral nervous system (the muscular and sensory organs).

Steady-state visual evoked potentials (SSVEPs) are the electrical responses of the brain to the flickering visual stimulus at a repetition rate higher than 6 Hz [4]. SSVEP-based BCI systems have advantage of easy-to-use and almost no user training thus becomes one of the popular paradigms in many applications. For instance, we proposed an SSVEP-based BCI system in which a user can make a phone call by gazing at the virtual keypad on a mobile device [5]. SSVEPs have also been used for clinical research and practice, e.g. migraine detection and/or prediction or seizure detection and monitoring [6][7]. Predicting or monitoring migraine attacks requires a user-acceptable, non-tethered, continuous and home-based SSVEP BCI system. Thus,

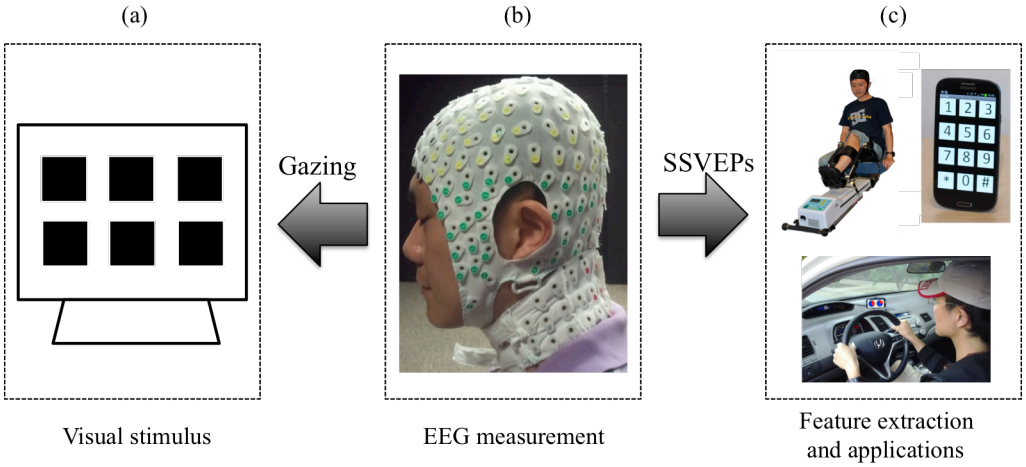

Figure 1.1 The basic design and operation of an SSVEP-based BCI system. (a) Visual stimulus. The visual stimulus could be rendered on a smartphone, a laptop or an LCD monitor. Each black square represents a target (commend) that is flickering at coded frequency or a pattern. For instance, one can specify each target as a number, a character, or a direction. (b) EEG measurement. The subject wore a 256 channels EEG cap and a 32 channels neckband to record the EEGs from the scalp and neck. When the subject was gazing at one target of the visual stimuli, the elicited SSVEPs can be collected, in general, from the occipital site over visual cortex. (c) Feature extraction and applications. The elicited SSVEPs can be converted to digital commends by feature extraction algorithms running in a device, such as a smartphone.

it is crucial to develop an SSVEP-based BCI system that is capable of delivering steady-state visual stimuli and continuously collecting and analyzing EEG data at the same time for either daily life or clinical research and practice.

Figure 1.1 shows the basic design and operation of an SSVEP-based BCI system in many applications. Depends on the applications and purposes, in general, we can divide the entire system into three basic components:

(A) Visual stimulus.

A good visual stimulus in a portable SSVEP-based BCI system relies on the mobility and the accuracy [8][9]. Several approaches have been carried out to elicit SSVEPs from the subjects. For instance, CRT based visual stimulators have been widely used in previous studies [10][11]. Gao et al. [12] used light-emitting diodes

(LEDs) to deliver visual stimuli in a BCI-based environmental controller. Shyu et al. [13] also designed a LED stimulation panel to display visual stimuli. Recently, liquid crystal display (LCD) based stimulators have become popular in SSVEP-based BCI systems [14].

Although different methods have been proposed in the design of visual stimulator for eliciting SSVEPs, the current visual stimulators are still very inconvenient and bulky. Users have to equip a computer monitor or an isolated visual stimulator (e.g. LEDs). The bulky SSVEP stimulator reduces the practicability of the BCI system, hindering the BCI applications. In short, although the SSVEP-based BCI has been well studied in the past decades, no one has implemented and integrated the visual stimuli and the near real-time EEG processing system in a single mobile device for ubiquity and portability.

(B) EEG measurement.

As SSVEPs are pre-dominantly originated from the visual cortex, it seems natural to collect the signals by placing electrodes over the occipital regions. Some studies even performed an off-line pilot experiment to obtain the optimal electrode locations prior to on-line BCI practices. However, no matter how people perform the EEG recording from hair-covered areas, they suffered from the complications of recording such as long preparation time and insufficient skin-electrode contact area due to hair. These complications make BCI impractical for routine use in daily life. To overcome these problems, dry contact- and non-contact-type EEG sensors have been

developed to enable user-friendly EEG measurements to improve the usability of BCI [15]-[19].

However, a major concern over the use of dry electrodes for EEG measurement is that the SNR of the acquired signals might not be as good as that from the gel based electrodes [15][16][18]. Furthermore, for some BCI users such as quadriparetic patients lying face up during ventilation, assessing the occipital sites would be undoubtedly more difficult either by wet or dry electrodes. Therefore, an alternative approach to easily extract high quality SSVEPs becomes a crucial issue in BCI community. The topography of SSVEP often shows a widespread scalp distribution because the SSVEP mainly projected from the visual cortex to the occipital areas, neck, forehead or even the face areas. Therefore, it's reasonable to believe that one could measure the SSVEP over non-hair-bearing areas. To our best knowledge, no study has yet systematically and quantitatively compared SSVEPs from different scalp and face locations using high-density EEG data.

(C) Signal processing platforms.

In real-life applications, BCI systems should not use bulky, expensive, wired EEG acquisition device and signal processing platforms [20]. Using these devices will not only cause discomfort and inconvenience for the users, but also affect their ability to perform routine tasks in real life. Recently, with advances in the biomedical sciences and electronic technologies, the development of a mobile and online BCI has been put on the agenda [19]. Several studies have demonstrated the use of portable devices for BCIs [13][19][20]. Lin et al. [20] proposed a portable BCI system that can

acquire and analyze EEG signals with a custom DSP module for real-time cognitive-state monitoring. Shyu et al. [13] proposed a system to combine an EEG acquisition circuit with an FPGA-based real-time signal processer. Recently, with the advances in integrated circuit technology, smartphones combined with DSP [21] and built-in Bluetooth function have become very popular in the consumer market. Compared with the PC-based or customized platforms, the ubiquity, mobility, and processing power of smartphones make them a potentially vital tool in creating on-line and portable BCIs that need real-time data transmission, signal processing, and feedback presentation in real-world environments.

Although the EEG-based BCI technology using PCs and the Bluetooth transmission of bio-signals have been well established in previous studies, the feasibility of a portable smartphone based BCI, which supports biomedical signal acquisition and on-line signal processing, has never been explored. This portable system emphasizes usability "on-the-go", and the freedom that smartphones enable. If a smartphone based BCI proves to be feasible, many current BCI demonstrations (e.g. gaming, text messaging, etc.) can be realized on smartphones in practice and numerous new applications might emerge.

In sum, three scientific and technical barriers need to be addressed when we would like to move an SSVEP-based BCI system from a laboratory demonstration to a real-life application: (1) the lack of precise visual stimulus presentation on mobile platforms; (2) the difficulty of assessing SSVEPs from easily accessible locations; (3)

the lack of a truly portable, user-acceptable (e.g. comfortable and wearable), and robust system for monitoring and processing EEG data from unconstrained users.

This thesis details and explores each component of an SSVEP-based BCI system from the front-end to back-end. We organize this thesis in the following way.

Chapter 2 describes state-of-art approaches of designing visual stimuli. We also propose a new way to render a frame rate-based visual stimulus without losing the accuracy and the portability. This approach was implemented on three different mobile devices, i.e. a smartphone, a Tablet, and a laptop to elicit SSVEPs. The feasibility of using a mobile stimulus presentation was suggested by the accuracy and stability of flickering frequencies and the elicited SSVEP signal in three subjects who participated in on-line SSVEP experiments.

Chapter 3 addresses a key issue of easy-of-use in real-world SSVEP-based BCI applications. More precisely, as SSVEPs are pre-dominantly originated from the visual cortex, it seems natural to collect the signals by electrodes placed over the occipital regions. Some studies even performed an off-line pilot experiment to obtain the optimal electrode locations prior to on-line BCI practices. However, no matter how people collect the EEG signals from hair-covered areas, they suffered from the complications of recording such as long preparation time and insufficient skin-electrode contact area due to the hair. These complications make BCIs impractical for routine use in daily life. Furthermore, for some BCI users such as quadriparetic patients lying face up during ventilation, assessing the occipital sites would be undoubtedly more difficult either by wet or dry electrodes. Therefore, an alternative

approach to easily extract high-quality SSVEPs becomes a crucial issue in the BCI community.

Chapter 4 proposes an approach to integrate a mobile and wireless EEG system and a real-time signal-processing platform based on a smartphone into a truly wearable and wireless online BCI. Its practicality and implications in routine use are demonstrated through the realization and testing of an SSVEP-based BCI.

Chapter 5 is a study that translates previous laboratory-oriented neurophysiological research to design, develop, and test an On-line Closed-loop Lapse Detection and Mitigation System featuring a mobile wireless dry-sensor EEG headgear and a smartphone based real-time EEG processing platform. Eleven subjects participated in an event-related lane-keeping task, in which they were instructed to manipulate a randomly deviated, fixed-speed cruising car on a 4-lane highway. The driving task was simulated in a 1st person view within an 8-screen and 8-projector immersive virtual-realty environment. When the subjects experienced lapses or failed to respond to lane-drift events during the experiments, auditory warning was delivered to mitigate the performance decrements.

Chatper 6 summaries the main contributions of this dissertation and discuss some future research directions.

Chapter 2

Developing Stimulus Presentation on Mobile Devices for a Truly Portable SSVEP-based BCI

In this chapter, we integrate visual stimulus presentation and near real-time data processing on a mobile device (e.g. a Tablet or a smartphone) to implement a steady-state visual evoked potentials (SSVEP)-based brain-computer interface (BCI). The goal of this study is to increase the practicability, portability and ubiquity of an SSVEP-based BCI for daily use. The accuracy of flickering frequencies on the mobile platforms was tested against that on a laptop/desktop used in our previous studies [5][8]. This study then analyzed the power spectrum density of the electroencephalogram signals elicited by the visual stimuli rendered on the mobile platforms. Finally, this study performed an online test with the Tablet-based BCI system and obtained an averaged information transfer rate of 33.87 bits/min in three subjects. The current integration leads to a truly practical and ubiquitous SSVEP-based BCI system on mobile devices for real-life applications.

2.1 BACKGROUND

In the past two decades, electroencephalogram (EEG)-based brain-computer interfaces (BCIs) have gained increasing attention in fields of neuroscience and neural engineering. While researchers have made significant progress in their efforts to design and demonstrate BCI systems, moving a BCI system from a laboratory demonstration to real-life applications still poses great challenges to the BCI community **[22]**[23].

Steady state visually evoked potential (SSVEP) [4] is a natural response to visual stimulation flickering at specific frequencies. It has been used for clinical research and practice, e.g. e.g. migraine, over 10% of the population (including children) suffers from migraine and it costs US more than $20 billion each year. [6][7]. Predicting or monitoring migraine attacks requires a user-acceptable, non-tethered, continuous and home-based SSVEP BCI system. Thus, a mobile device that can deliver steady-state visual stimuli and continuously collect and analyze EEG data at the same time is crucial for clinical applications such as migraine and seizure detection and monitoring.

Our recent study [5] demonstrated a smartphone based BCI that took advantage of the robust SSVEP. The entire system consisted of three parts: (1) a near real-time data processing platform (e.g., a Bluetooth-enabled smartphone or a Tablet), (2) a mobile and wireless EEG device (e.g., a customized EEG headband featuring Bluetooth module, amplifier circuits, and a microprocessor), and (3) a computer screen (e.g., a cathode ray tube (CRT) monitor). Though the smartphone based EEG acquisition and near real-time data processing significantly increased the portability of

an EEG system in the BCIs, the SSVEP-based BCI system was still not completely portable or ubiquitous because subjects have to equip a bulky screen for stimulus presentation.

Several approaches have been carried out to elicit SSVEPs from the subjects. For instance, CRT based visual stimulators have been widely used in previous studies [10][11]. Gao et al. [12] used light-emitting diodes (LEDs) to deliver visual stimuli in a BCI-based environmental controller. Shyu et al. [13] also designed a LED stimulation panel to display visual stimuli. Recently, liquid crystal display (LCD) based stimulators have become popular in SSVEP BCIs [14]. Although different methods have been proposed in the design of visual stimulator for eliciting SSVEPs, the current visual stimulators are still very inconvenient and bulky. Users have to equip a computer monitor or an isolated visual stimulator (e.g. LEDs). The bulky SSVEP stimulator reduces the practicability of the BCI system, hindering the BCI applications.

In short, although the SSVEP-based BCI has been well studied in the past decades, no one has implemented and integrated the visual stimuli and the near real-time EEG processing system in a single mobile device for ubiquity and portability.

This study proposes to implement the display of visual stimulus together with near real-time data processing in a single mobile and wireless device, such as a laptop, a Tablet, or even a smartphone. Since the smartphone or Tablet based online EEG processing has been reported in detail in our previous study [5], this study then focuses on the implementation, integration, and validation of the SSVEP stimulus presentation on a portable device. This study first examines the accuracy and stability of visual

stimulus rendered on each device, and then evaluates the all-in-one SSVEP BCI by analyzing the power spectrum density (PSD) of the EEG recorded from three healthy subjects performing the SSVEP experiments. Finally, this study performs an online test with three subjects to evaluate the performance of a Tablet-based BCI. The goal of this study is to demonstrate the feasibility of eliciting reliable SSVEPs and processing the wirelessly acquired EEG data on a single mobile device. The results of this study may lead to a truly practical and ubiquitous SSVEP BCI for daily use.

2.2 METHOD

In this Section, we first describe three common paradigms to deliver the visual stimuli for the SSVEP-based BCI systems. According to the purposes or the domains of use, each paradigm has its advantage and disadvantages over others. A frame-rate based approach to render the visual stimuli is also covered. Second, we systematically and quantitatively compare the accuracy of frame rate-based visual stimuli on different mobile platforms. Finally, we collected EEG data from three subjects who participated in the on-line experiments to test the accuracy of elicited SSVEPs.

2.2.1 THE DESIGN OF VISUAL STIMULI

The visual stimulus is one of the main components in the SSVEP-based BCI systems. Several factors, such as the flickering accuracy, portability, and re-configurability, need be concerned when designing visual stimuli in the system. In this section, we first address the background of VEPs and SSVEPs, and diversities of stimulators. Then, we address three basic visual stimuli paradigm: time-modulated

visual evoked potentials (tVEPs), frequency-modulated visual evoked potentials (fVEPs), and code-modulated visual evoked potentials (cVEPs). Finally, we present a new approach for rendering fVEPs-based visual stimuli on three portable platforms.

(A) VEPs, SSVEPs, and Stimulators

VEPs are the positive and negative voltage oscillation responses to visual stimuli such as light, appearance of an image or abrupt change of color or pattern **[4]**. Steady-state VEPs are created by the stable VEPs oscillation that is elicited by rapid repetitive stimulation. The visual stimulus plays a very important role in the success of an SSVEP-based BCI system.

Visual stimuli can be presented using flashing lights or LEDs **[12]**, or flickering targets on a computer screen **[5]**. Cheng et al. **[24]** proposed an SSVEP-based BCI system by applying 4 flickering LEDs ranging from 6Hz to 9 Hz at each corner of a screen. When subjects fixated on one of the blocks, their SSVEPs would include the harmonic components of the corresponding flash frequency. The block could then be chosen by analysis of the EEG data. According to the analysis results, the cursor and the blocks would be moved together in corresponding directions. Wang et al **[5]** proposed a smartphone-based SSVEP system that used CRT to render visual stimuli to elicit SSVEPs. When subjects selected ten digits by gazing each flickering target, the smartphone dials the number automatically. Wu et al. **[25]** showed the comparison of visual stimuli rendered by LEDs, CRT, and LCD and the elicited SSVEPs. A remarkable result was that the elicited SSVEPs by CRT had higher harmonic. In general, the amplitude ranking of elicited SSVEPs is LEDs > CRT~=LCD with 10.8Hz

visual stimuli, and almost the same for the other two frequencies (4.6Hz and 16.1Hz). This result suggests that LEDs are the best stimulator to elicit SSVEPs. However, if considering stimulation parameters such as size, color and position, presenting flickers on a computer monitor is a more flexible approach than using stand-alone dedicated lights or LEDs. For instance, one can easily reconfigure the shape, color, and number of targets rendering on the monitor while LEDs might take longer setup time.

(B) Visual Stimuli Paradigms

The visual stimuli have three basic paradigms to render on the screen: time-modulated, code-modulated, and frequency-modulated **[26]**. In t-VEPs paradigm, the different stimuli have mutual flickering sequences; in the c-VEPs paradigm, each stimulus uses pseudorandom sequences; in the f-VEPs paradigm, each stimulus is coded and flickering at specific frequency. Figure 2.1 shows three paradigms of visual stimuli. In t-VEPs, as shown in Figure 2.1(a), we can see that the "stimuli on" (trace high) among all targets are mutually exclusive across time. In f-VEPs, as shown in Figure 2.1(b), the "stimuli on" on each target presents at specific frequency. Note that the elicited SSVEPs are consisted of the fundamental (~10Hz) and harmonic (~20Hz, ~30Hz, etc.) frequencies in this paradigm. Figure 2.1(c) shows the pseudorandom sequence rotating 4 bits to the right for each target such that each target is near orthogonal. Bin et al. [26] compared the information transfer rates (ITRs) [1] when three different paradigms were presented. The results showed that the c-VEPs paradigm performed best, followed by the f-VEPs paradigm, and then t-VEPs paradigm. Although the f-VEP paradigm couldn't produce the best ITRs, the advantage of not

requiring time- or phase- locked recording is very appealing in real-life environments. Over the past 12 years, standard (f-VEPs) SSVEP-based BCI systems have gained a lot of attention due to less training and high ITR **[27]**. In f-VEPs paradigm, most studies use screen refresh rate to render the visual stimuli **[27]**-**[30]**. When using this approach to ensure a flicker's frequency stability, the number of stimuli is always limited by the refresh rate of a monitor. For example, on a monitor with a 60 Hz refresh rate, the usable stimulus frequencies within the EEG alpha band (8-13 Hz) can only be at 8.57 Hz (7 frames per period), 10 Hz (6 frames per period) and 12 Hz (5 frames per period), where 1 frame is 1/60 second. In other words, multiple targets (more than three) can't be achieved by this method. For instance, We proposed a phone dialing system requires at least 12 targets (10 digits, backspace, and confirm) to function **[5]**. In an SSVEP-based BCI system the performance is highly affected by the number of targets. The ITR can be improved with an increased number of targets. Currently, the visual stimulator design is one of the limiting factors of SSVEP-based BCI systems. An alternative approach is to program stimulus presentation using high-resolution timers such as the Windows Multimedia Timer **[31]**, i.e. acquiring the system clock to render the stimuli. However, when using a timer, the frequency resolution is limited by the timer's error affected by other active Windows processes.

(C) Approximated Visual Stimuli Design

In conventional refresh-rate-based stimulus designs, the number of frames in each cycle is constant. For instance, to produce a 10 Hz flicker with a 60 Hz refresh rate, the stimulus pattern reverses between black and white every three frames,

asshown in Figure 2.1 (a). In this regime, it is impractical to generate an 11 Hz stimulus because mathematically the stimulus presentation should reverse every 2.73 frames, as shown in Figure 2.1 (c). Wang et al **[8]** proposed to approximate this presentation rate using a varying number of frames in each cycle (five or six, corresponding to 12 and 10 Hz, respectively). Figure 2.2(d) shows a sequence for an 11 Hz stimulus. Generally, the stimulus signal at frequency f can be calculated as follows:

$$stim(f,i) = square\left[2pf\left(\frac{i}{RefreshRate}\right)\right] \quad (2.1)$$

where *square(2pft)* generates a square wave with frequency *f*, and i is the frame index. As shown in Figure 2.2(d), in a 0.2 second stimulus sequence, the black/white reversing interval for the 11 Hz stimulus is: [2 2 3 3 3 2 2 2 3 3], which includes 10 cycles with a varying length of two or three frames. Based on this approach, a stimulus at any frequency up to half of the refresh rate can be realized.

2.2.2 THE PLATFORMS OF RENDERING VISUAL STIMULI

Three portable platforms were selected to deliver the visual stimuli of an SSVEP-based BCI system: a laptop (Lenovo X200S), a Tablet (Motorola XOOM), and a smartphone (Samsung Galaxy S). Table 2.1 lists the specifications of three devices. The flickering visual stimulation displayed on a laptop running Microsoft Windows operation system has been implemented and demonstrated in our previous study [5]. This section therefore only describes the details of the design and implementation of stimulus presentation on Android based mobile devices. For presenting SSVEP visual

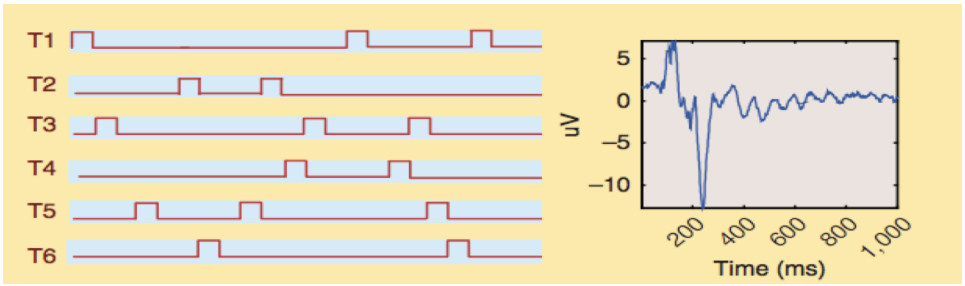

(a)

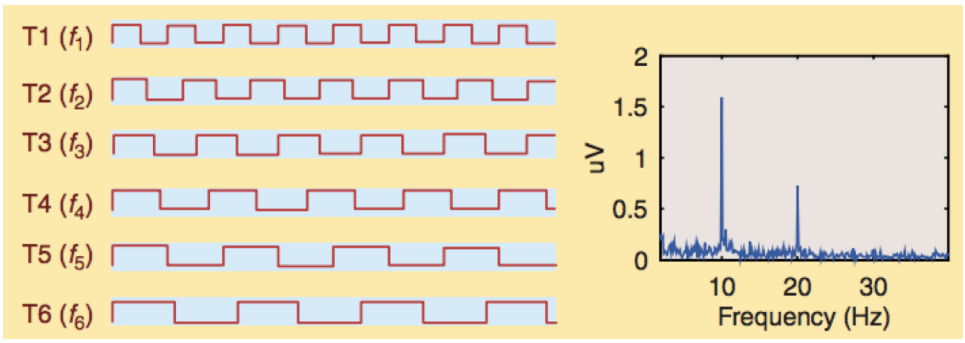

(b)

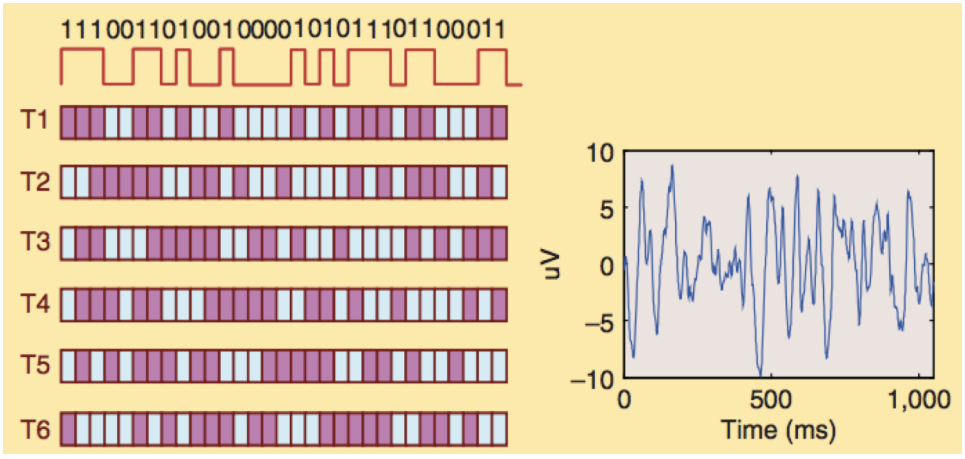

(c)

Figure 2.1 The three common visual stimuli paradigms. Note that, T1-T6 represent target 1 to target 6. (a) t-VEPs. The high trace for each target indicates the stimulus being turned on, while low trace indicates the stimulus turns off. Right panel represents the elicited VEPs consisted of positive (~100ms) and negative (~250ms) voltage deflections. (b) f-VEPs. The stimulus on/off frequency of each target is different. Right panel indicates the power spectrum density of elicited VEPs when the subject was gazing at a target flickering at 10Hz. This example also shows its harmonic frequencies (20Hz). (c) c-VEPs. A pseudorandom sequence (top left) was shifted 4bits right for each target. Right panel indicates an example of the elicited VEPs when the subject was gazing at one target. This figure is reprinted with permission from [26].

Table 2.1 The specifications of visual stimulators.

	Lenovo X200s	**Motorola XOOM**	**Samsung Galaxy S**
OS	Windows XP SP3	Android 3.0	Android 2.1
CPU	Intel Core 2 Duo 1.4GHz	NVIDIA Tegra 2 Dual-Core 1GHz	ARM Cortex-A8 1 GHz
Software	Direct X	OpenGL ES	OpenGL ES
Screen refresh rate (Hz)	60.375	59.975	55.575
Screen size (inch)	13	10.1	4
Screen resolution (pixels)	800 × 1280	800 × 1280	400 × 800

stimuli on a portable device, the stability of screen refresh rate is very important. This study first tests the screen refresh rate with a silicon NPN phototransistor (PNA1605F). The three devices have different refresh rates: 60.375Hz for the laptop, 59.975Hz for the Tablet, and 55.575Hz for the smartphone.

2.2.3 SOFTWARE ARCHITECTURE

The application of visual stimulation was written in Java under Eclipse integrate development environment. An Android Development Tools plugin to Eclipse facilitates the development and deployment of Android applications across different platforms. Figure 2.3 shows the flowchart of the program delivering flickering visual stimulus. The OpenGL ES (OpenGL for embedded system, version 1.0) technology was used to realize a frame-based display. The stimulation application can display one or multiple

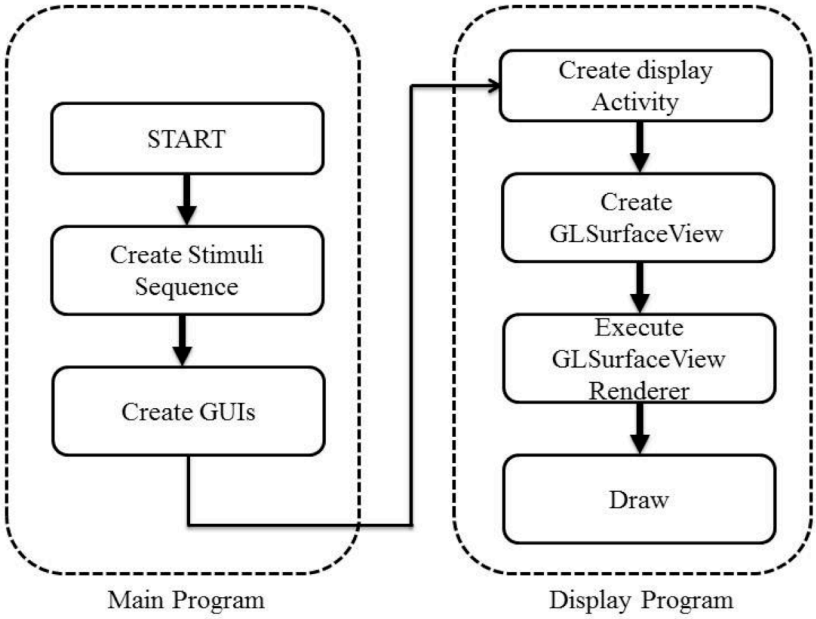

Figure 2.2 The flowchart of visual stimulus program. The stimulation software consists of two saperate threads: Main Program and Display Program. Main Program goes to sleep mode and the screen starts to render the visual stimuli after Create GUIs is done.

flickering 3.5cm × 3.5cm squares on the screen over a black background according the screen resolution, accomplished by sequential rendering of black and white colors at a specific frequency [8].

The application of visual stimulus consists of two major threads, as shown in Figure 2.3. The Main Program is responsible for creating graphic user interfaces and calculating the stimulation sequence under a specific screen refresh rate. According to the approach proposed in [8], the stimulation sequence may vary due to the screen refresh rate. For instance, displaying an 11Hz flickering square on the screen refreshed at 60 Hz can be realized with 11-cycle black/white alternating patterns lasting [3 3 3 2 3 3 3 2 3 3 2 3 3 3 2 3 3 3 2 3 3 2] frames in a second. On the other hand, the Display Program is responsible for rendering the flickering animation. GLSurfaceView, a class

of Android.opengl makes it possible to draw flickering animation frame-by-frame by creating and managing a separate thread. In general, multiple flickers flickering at different frequencies can be implemented at the same time.

2.2.4 PLATFORM TESTING AND EEG EXPERIMENT

In order to test the stability of the flicker on each platform, the silicon NPN phototransistor was directly attached to the center of the flickering animation on the screen to examine the quality of the flickering stimulation. For each platform, 11Hz flickering stimuli (one minute long) were recorded using an EEG amplifier. The EEG amplifier is a 16-channel bio-signal acquisition unit. Signals within the frequency band of 0-250 Hz were amplified and digitized by analog-to-digital converters (ADC) with a 24-bit resolution at a sampling rate of 1000 Hz.

To further validate the usability of each platform for eliciting SSVEPs, an EEG experiment was conducted on three subjects. Two of them were naive subjects to the SSVEP experiment (subjects 2 and 3), while subject 1 has experience in using an SSVEP-based BCI. Each subject repeated this task on each of the three platforms. The goal of this testing is to verify the presence of the 11Hz brain activity induced by the visual stimulus. During the SSVEP experiments, the subjects gazed at a single flicker animation flashing at 11Hz for one minute with no feedback. EEG signals were recorded from two electrodes placed over the occipital region, referenced to the forehead. The channel with higher signal-to-noise ratio (SNR) was selected for further analysis.

2.2.5 DATA ANALYSIS

The flickering animation signals rendered on the three different platforms were recorded and filtered with a (8-20 Hz) band-pass filter. Secondly, one-minute recording was partitioned into fifteen 4-sec trials. Fast Fourier Transform (FFT) was then applied to the averaged waveforms of the segmented data and the resultant PSDs were plotted to evaluate the flickering frequencies on different platforms and elicited SSVEPs.

2.2.6 ON-LINE TESTING

A Tablet-based system integrating visual stimulus presentation and data processing was tested on an online BCI experiment. Three subjects performed a phone-dialing task, in which they need to dial 10-digit numbers using their brain activities as described in [5]. An EEG headband, which features miniature amplifier, Bluetooth module, and a microprocessor [5], was used for data collection. A virtual keypad comprised 12 targets on the screen of the Tablet. Each target was a 3.5cm × 3.5 cm square. The frequencies ranged from 9-11.5Hz with a 0.25Hz interval. Each subject sat in a comfortable chair in a dim room. The Tablet was placed ~60cm in front of them. They were asked to gaze at the targets sequentially with the following sequence: #, 1, 2, 3, 4, 5, 6, 7, 8, 9, 0, #. The SSVEP frequencies in the 4-channel EEG from the headband were detected by the canonical correlation analysis (CCA) algorithm [14]. The target stimulus on the screen would change to a red background (as visual feedback) for about 200ms once the target had been identified. The subject was

instructed to switch to the next target immediately following the feedback. Each subject repeated the task five times and the averaged ITR was used to evaluate the BCI performance.

2.3 RESULTS

In this Section, we first verified the accuracy of the visual stimuli by attaching a phototransistor on the screen of mobile devices. Second, we collected EEG data from three subjects while they were performing the on-line experiments to test the accuracy of elicited SSVEPs.

2.3.1 ACCURACY AND STABILITY OF FLICKERING SIGNALS

Figure 2.3 shows the averaged time series and PSDs of the acquired flickering animations from three different platforms. The stimulus signals (Figure 2.3 (a)) on the laptop and the Tablet are more stable than those rendered on the smartphone. More precisely, the signal waveforms flashed from the laptop and the Tablet had almost same phases in each second, while the phase of 11Hz stimulus signals on the smartphone shifted back and forth slightly. The normalized PSD (Figure 2.3 (b)) shows that the stimulus signal on all platforms contained the correct fundamental frequency (11Hz). The normalized amplitude of the stimulation frequency on the smartphone is smaller than that of other platforms due to the phase jitter of the screen

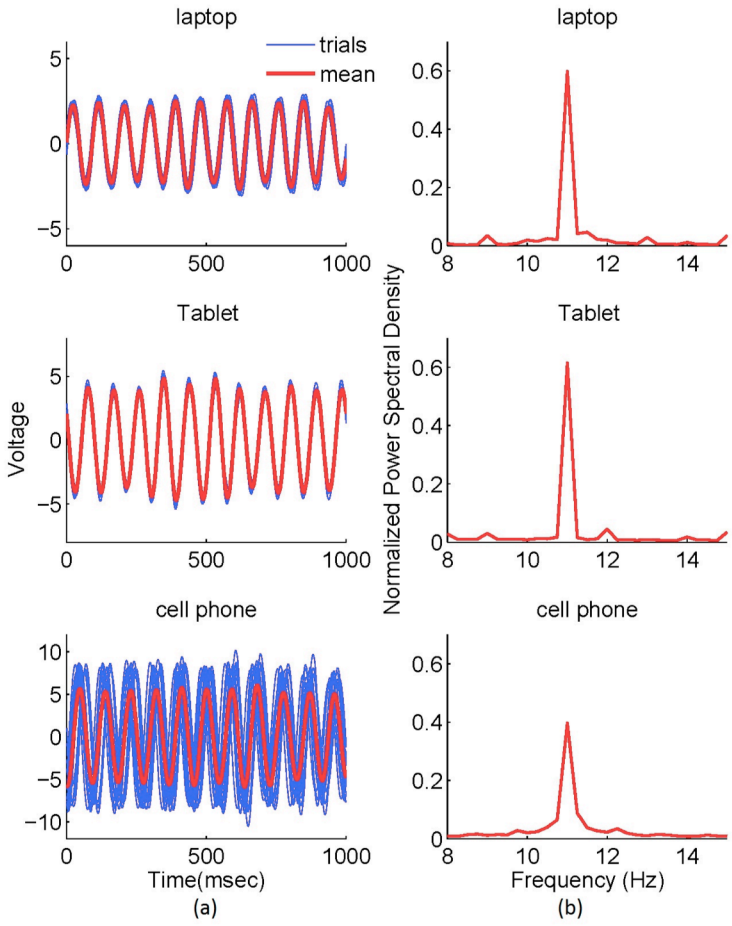

Figure 2.3 The waveforms and power spectra of the flickering signals. (a) Time series of averaged flickering signals from the laptop, the Tablet and the smartphone. (b) The normalized power spectral density of the flickering signal on each platform.

refresh rate. Although the flickering signal on the smartphone is not as stable as other platforms, the stimulation frequency is still accurate.

2.3.2 SSVEP SIGNALS

Figure 2.4 shows the averaged SSVEPs and their PSDs elicited by the flickering stimuli on the three platforms for all the subjects. Figure 2.4 (a) exhibits characteristic sinusoidal SSVEPs. Because the stimulus signal and the EEG signal were not synchronized, SSVEPs of the three subjects had different initial phases. Figure 2.4 (b) plots the PSDs of SSVEPs elicited by the flickering stimuli, all showing very consistent and accurate 11Hz peaks. For all subjects, the amplitudes of the 11Hz SSVEPs elicited by the laptop and Tablet screens were higher than those elicited by the smartphone.

Table 2.2 On-line ITR testing results among three subjects.

Experiment run	Subject 1	Subject 2	Subject 3
1	49.64	28.13	31.15
2	45.66	35.76	22.54
3	41.64	25.17	33.26
4	50.74	29.89	25.05
5	49.64	20.99	18.74
Average	47.46	27.99	26.15
Standard deviation	±3.39	±4.92	±5.38

2.3.3 ON-LINE RESULTS

The ITR in bits/minute was calculated as follows [1]:

$$\text{ITR} = log_2 N \ + A\ log_2 A + (1 - A) log_2 \left[\frac{1-A}{N-1}\right] \tag{2.2}$$

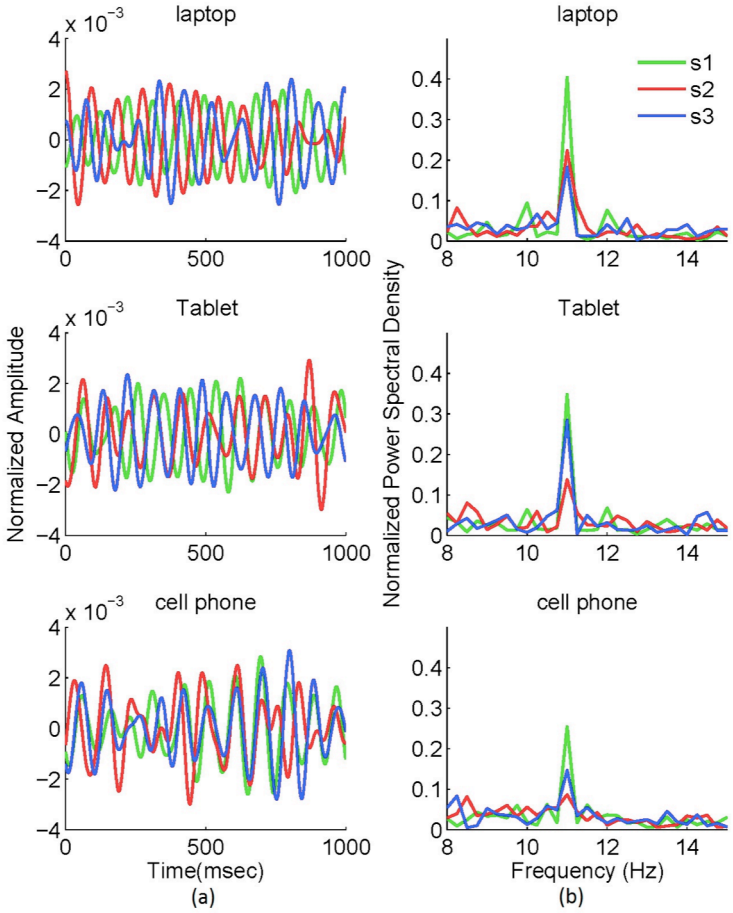

Figure 2.4 EEG signal acquired and averaged during visual stimulation presenting with a frequency of 11 Hz and its power spectrum. (a) Sample SSVEP signal obtained from the three subjects on different platforms. (b) The frequency spectrum corresponding to the signal in left. The SSVEP manifests itself in oscillations at 11 Hz.

where N is the number of targets, and A is the accuracy of frequency detection. Table 2.2 shows the ITR in bits/minute for all subjects. All subjects fulfilled the tasks. The averaged ITR is 33.87 bits/min, which is comparable to previous studies using a separate stimulating device [5][10].

2.4 CONCLUSION

This study implemented and demonstrated a practical and ubiquitous SSVEP-based BCI system for real-world applications. The feasibility of using a mobile stimulus presentation was suggested by the accuracy and stability of flickering frequencies and the elicited SSVEP signals. As the feasibility of using a mobile device (a smartphone or a Tablet) to acquire and process EEG signals from unconstrained individuals in real-world environments has been demonstrated in our previous studies [5][8], the integration of stimulus presentation and real-time data analysis on a single mobile device leads to a truly practical, online SSVEP-based BCI for real-life applications that require continuous and ubiquitous monitoring of the brain.

ACKNOWLEDGEMENTS

This chapter contains material from "Developing Stimulus Presentation on Mobile Devices for a truly Portable SSVEP-based BCI" by Yu-Te Wang, Yijun Wang, Chung-Kuan Cheng, and Tzyy-Ping Jung, which appears in the *35th Annual International Conference of the IEEE Engineering in Medicine and Biology Society (IEEE EMBC 2013)*. The dissertation author was the first investigator and author of this paper.

Chapter 3

Measuring Stead-State Visual Evoked Potentials from Non-hair-bearing Areas

Steady-State Visual Evoked Potential (SSVEP)-based Brain-Computer Interface (BCI) applications have been widely applied in laboratories around the world in the recent years. Many studies have shown that the best locations to acquire SSVEPs were from the occipital areas of the scalp. However, for some BCI users such as quadriparetic patients lying face up during ventilation, it is difficult to access the occipital sites. Even for the healthy BCI users, acquiring good-quality EEG signals from the hair-covered occipital sites is inevitably more difficult because it requires skin preparation by a skilled technician and conductive gel usage. Therefore, finding an alternative approach to effectively extract high-quality SSVEPs for BCI practice is highly desirable. Since the non-hair-bearing scalp regions are more accessible by all different types of EEG sensors, this study systematically and quantitatively investigated the feasibility of measuring SSVEPs from non-hair-bearing regions, compared to those measured from the occipital areas. Empirical results showed that the signal quality of the SSVEPs from non-hair-bearing areas was comparable with, if

not better than, that measured from hair-covered occipital areas. These results may significantly improve the practicality of a BCI system in real-life applications; especially used in conjunction with newly available dry EEG sensors.

3.1 BACKGROUND

SSVEP is the electrical response of the brain to flickering visual stimuli. SSVEP-based BCI recently has been widely used in many applications due to its advantages such as little user training and high information transfer rate [32]. For example, Gao et al. [12] applied the SSVEP to the control of electric apparatus that featured noninvasive signal recording, little training requirement, and a high information transfer rate. As a result, more studies have explored applications of this technology.

As SSVEPs are pre-dominantly originated from the visual cortex, it seems natural to collect the signals by placing electrodes over the occipital regions. Some studies even performed an off-line pilot experiment to obtain the optimal electrode locations prior to on-line BCI practices. However, no matter how people perform the EEG recording from hair-covered areas, they suffered from the complications of recording such as long preparation time and insufficient skin-electrode contact area due to hair. These complications make BCI impractical for routine use in daily life. To overcome these problems, dry contact- and non-contact-type EEG sensors have been developed to enable user-friendly EEG measurements to improve the usability of BCI. However, a major concern over the use of dry electrodes for EEG measurement is that the SNR of the acquired signals might not be as good as that from the gel based

electrodes [15][16][18][33]. Furthermore, for some BCI users such as quadriparetic patients lying face up during ventilation, assessing the occipital sites would be undoubtedly more difficult either by wet or dry electrodes. Therefore, an alternative approach to easily extract high quality SSVEPs becomes a crucial issue in BCI community.

The topography of SSVEP often shows a widespread scalp distribution because the SSVEP mainly projected from the visual cortex to the occipital areas, neck, forehead or even the face areas. Therefore, it's reasonable to believe that one could measure the SSVEP over non-hair-bearing areas. To our best knowledge, no study has yet systematically and quantitatively compared SSVEPs from different scalp and face locations using high-density EEG data. This study aims to answer two main questions: (1) Can SSVEP be measured from non-hair-bearing areas? What is the quality of the signals compared against that from the hair-covered area? (2) How many channels of non-hair-bearing SSVEP data would be needed to archive the same SNR measured from the occipital areas in SSVEP experiments? If the proposed non-hair-bearing montage approves feasible, the practicality of an SSVEP BCI system can be significantly improved, especially used in conjunction with dry EEG sensors such as non-contact [18] or polymer based electrodes [15].

3.2 METHODS

Brain activities can be acquired invasively or noninvasively. Invasive measurement involves brain surgery that is not acceptable for healthy subjects. Noninvasive measurement, such as PET, MRI, and MEG, are usually expensive,

constrained and impractical in real-life environments. Bridging the gap between laboratory demonstration and real-life applications remains a challenge in the BCI community. EEG measures the voltage fluctuations within the neurons of the brain as projected onto the scalp. The measurement devices are inexpensive, convenient, and amenable to diverse environments. There are several commercial products featuring portability, wireless capability and low cost for wide variety of purposes **[5][34][35]**. EEG therefore seems to be a reasonable alternative for daily use. In this section, we cover the basic hardware design for measuring EEG from the scalp as well as a simple overview of diverse electrodes. Finally we address a neurological study exploring different approaches to collect EEG.

3.2.1 STIMULI AND PROCEDURE

The visual stimulus was a 5 x 5 cm square coded and rendered at the center of a 21" CRT monitor with a 120Hz refresh rate. The stimulus frequencies ranged from 9Hz to 13Hz with an interval of 1Hz. In general, this cannot be implemented with a fixed rate of black/white flickering pattern due to a limited refresh rate of a LCD screen. Wang et al. [8] developed a method that approximates target frequencies of SSVEP BCI with variable black/white reversing intervals. Based on this approach, any stimulus frequency up to half of the refresh rate of the screen can be realized. The stimulus program was developed in Microsoft Visual C++ using the Microsoft DirectX 9.0 framework and rendered on Windows XP platform.

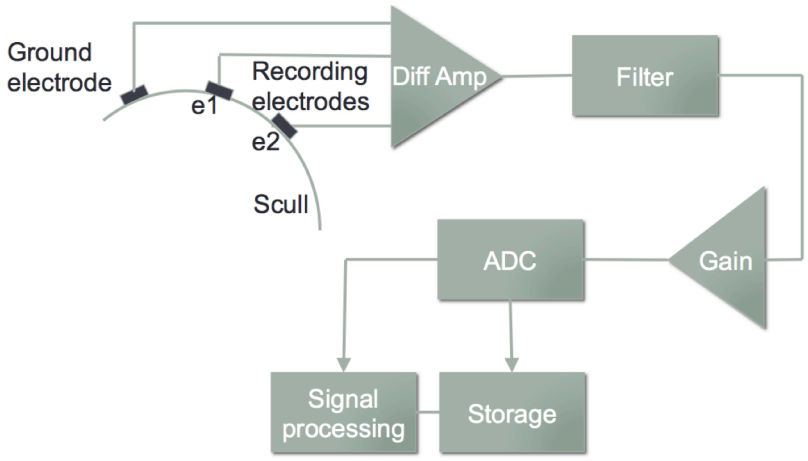

Figure 3.1 The function blocks of an EEG recording system, adapted from [36]. Note that, Diff Amp stands for differential amplifier, and ADC stands for analog-to-digital conversion.

Subjects were seated in a comfortable chair in front of the monitor. A chin rest was used to fix the head 35 cm from the screen. The experiment consisted of four sessions, each including five 30s-long trials for the five different stimulus frequencies, which were randomly presented. Subjects were asked to gaze on the flickering stimulus for 30 seconds and then take a ~15s rest after each trial in order to avoid visual fatigue caused by flickering. There was a several-minute break between two sessions.

3.2.2 DATA ACQUISITION

(A) Basic Electronic Property

Figure 3.1 depicts the major components of an EEG recording system. The ground electrode is connected to the ground of differential amplifier that is isolated from line power. Two recording electrodes, e1 and e2, measure the potential of two

sites of scalp with respect to the common ground. The differential amplifier can eliminate the common-mode potential and amplifies the potential of two recording electrodes' sites. The amplified signals are then filtered and substantially amplified by the gain amplifier. Here, the filter could be a notch filter to reject line noise, or high-pass, log-pass filters. The gain amplifier substantially amplifies the signal (e.g., amplified by a factor of 10,000). Next, the ADC digitalizes the signal for further signal processing or storage.

(B) Wet and Dry Electrodes

In the most-recent BCI systems, sensors also play an important role in term of obtaining high quality EEG signals [16][18][33]. Ag/AgCl (silver/silver-chloride) electrodes (also known as wet electrodes) have been used for many years for collecting EEG noninvasively. During experiment preparation, skilled technicians usually abrade the scalp at the electrode site and apply conductive gel between scalp and electrode in order to degrade the impedances (usually less than 10K ohm). Another wet-like electrode is a sponge-saline electrode [34]. The sponge absorbs saline water and attaches directly on the scalp before an experiment. Although the impedance of sponge-saline electrodes is higher than that of the conductive gel electrodes, the advantages of short time preparation and easily washing after an experiment makes it acceptable to subjects. As a result, although wet sensors have low impendence because of the conductive gel that is applied, it still suffers drawbacks such as non-reconfigurability, not easily washable, lack of ease-of-use.

Another type of electrodes, dry electrodes, requires no conductive material between scalp and electrodes [15][16][18][19]. Chou et al. [16] developed a Micro-Electro-Mechanical Systems (MEMS)-based silicon spiked electrode array to collect EEGs. This sensor penetrates the stratum corneum of the skin and obtains superior electrically conducting characteristics without requiring conduct gel on the skin. However, the authors didn't mention the endurance and fragility of the sensors in that study, such as whether the tip could break off [17]. An alternate dry electrode, g.SAHARA, developed by g.tec [35], is consisted of eight probes made of special golden alloy within a male snap-in button. Each probe has sufficient length to go through the hair to reach the scalp. Chi et al [18] developed noncontact sensors that operate primarily through capacitive coupling. All of these sensors prove the ability to collect EEGs noninvasively when connected with specific hardware. As a result, although dry sensors have many advantages, including little preparation time and washing needed, ease-of-use, and reconfigurability, the problem of reducing the high impendence remains.

As SSVEPs predominantly originate in the visual cortex, it seems natural to collect the SSVEP signals by placing wet/dry electrodes on the occipital regions over visual cortex. Some studies even performed an off-line pilot experiment to obtain the optimal electrode locations prior to on-line BCI practices [14][30]. However, no matter how people perform the EEG recording from hair-covered areas, they still suffer from complications such as skin preparation and insufficient skin-electrode contact area due to hair. These complications make BCI impractical for routine use in daily life. To

overcome these problems, dry contact- and non-contact-type EEG sensors have been developed to enable user-friendly EEG measurements to improve the usability of BCIs [18][19]. However, a major concern over the use of dry electrodes for EEG measurement is that the SNR of the acquired signals might not be as good as that from the gel based electrodes BCIs [18][19]. Furthermore, for some BCI users such as quadriplegic patients lying face up during ventilation, assessing the occipital sites are undoubtedly more difficult either by wet or dry electrodes. Therefore, an alternative approach to extract high quality SSVEPs becomes a crucial issue in BCI community.

Five healthy male subjects with normal or corrected to normal vision participated in this experiment. All participants were asked to read and sign an informed consent form approved by the UCSD Human Research Protections Program before participating in the study.

EEG data were recorded using Ag/AgCl electrodes from 256 locations distributed over the entire head using a BioSemi ActiveTwo EEG system (Biosemi, Inc.). Figure 3.2 shows the 256-channel cap that covers not only the brain areas, but also the non-hair-bearing areas including the forehead, face, behind-the-ear, and neck areas. Additional bipolar horizontal and vertical EOG electrodes monitored eye movements. Electrode locations were measured with a 3-D digitizer system (Polhemus, Inc.). All signals were amplified and digitized at a sample rate of 2,048 Hz. All electrodes were with reference to the nasion.

3.2.3 EEG DATA PRE-PROCESSING

The 256-channel EEG data were first down-sampled to 256Hz. For each trial, six 4s-long EEG epochs were extracted according to event codes generated by the stimulus-presentation program [8]. For each stimulus frequency, the epochs from the four sessions were concatenated to form a dataset of 24 epochs. Epochs with severe artifacts (such as movement artifacts and eye blinks) were manually removed from the dataset. To remove the spontaneous EEG activities, the remaining epochs were averaged to obtain the multi-channel SSVEP signals.

3.3 SIGNAL PROCESSING ALGORITHMS

The purpose of applying any signal-processing algorithms on the collected EEG signals is to extract useful information for further use. This process is also called feature extraction. Depending on the different applications and domain of use, one can select specific some algorithms to maximize the performance of their system. For instance, the Oddball Paradigm experiments usually average the time-domain EEGs across different trials to explore the positive/negative deflection after a stimulus delivered under a specific set of events [37]. In this section we address several useful methods to extract SSVEP signals.

(A) Noise, artifact, fundamental signal, and signal to noise ratio

The term ‘noise’ usually refers to spontaneous neurological activities found in the background of the EEG recording. In contrast, artifacts are the unexpected signal

that is unrelated to brain activity, such as eye blinks. Both of them can contaminate the fundamental signal.

When we apply algorithms to extract useful information from the collected EEGs, we have to know what kind of signal is needed. In the most-recent SSVEP-based BCI systems with frequency-modulation-based visual stimuli, the visual stimuli are likely, but not limited to, coded at range of alpha-waves (8-13Hz) due to the fact that one can obtain highest SNR and highest amplitude response [30]. The fundamental signals of interest in an SSVEP-based BCI system are the signals in the alpha band elicited by the visual stimuli.

Signal to noise ration (SNR) can be interpreted the ratio of fundamental signal power to the noise power [38]. As mentioned in the last paragraph, one can arbitrarily define the frequency range of the fundamental signal and noise, and evaluate the SNR by squaring the amplitude after FFT. In general, a high SNR indicates the data contains low noise. This study used SNR to evaluate the quality of SSVEPs. Fast Fourier Transform (FFT) was used to calculate the amplitude spectrum of the 4s-long EEG data (i.e., y=|FFT(x)|). The frequency resolution of the resulting amplitude spectrum was 0.25Hz. The SNR was defined as the ratio of the amplitude of the SSVEP (at the stimulating frequency) to the mean amplitude of the background noise (within the frequency band of 8-15Hz, which includes 28 frequency bins)

$$SNR = \frac{28 \times y(f)}{\sum_{k=8}^{15} y(k) - y(f)}, \text{ where } k \neq f \qquad (3.1)$$

(B) Fast Fourier Transform (FFT)

FFT is a very useful function to convert the signal from the time domain into its equivalent frequency domain representation. When we applied this approach on SSVEPs, the collected signals are decomposed into individual sinusoidal components that can be recognized and evaluated independently.

(C) Principle component analysis (PCA)

PCA is used to find the dominant component that consists of the linear combination from the original data set and the weight matrix. In other word, PCA finds a square weight set W that transfers the EEG data set X into a new data set Y with the same dimension, such that the first principal component of new data set Y is the linear combination of the EEG data set X with maximum amplitude variance. Note that, the first principal component may or may not the desired signal. For instance, the original data set were contaminated by strong line nose while recording, the first dominant decomposed signal is very likely line nose instead of SSVEPs.

(D) Independent component analysis (ICA)

ICA is one of the successful statistic approaches used to separate the EEG signals into independent neurological activities and other noises [39]. Consider an EEG data set X composed of independent source S in which X=AS, where A is a mixing matrix. After applying ICA, a recovered source U is composed of a spatial filter matrix W times X, i.e. U=WX. The detailed explanation of infomax ICA can be found in [39]-[43]. In general, ICA is relatively complex algorithm and presents a significant challenge in real-time BCI applications [38].

(E) Canonical Correlation Analysis

Canonical Correlation Analysis (CCA) has the ability to find two basis vectors of different data sets, such that the projection of the original data set to the basis vectors is maximally correlated. For instance, consider the two data sets x and y that can be represented by $X = w_x^T x$, and $Y = w_y^T y$ where w_x^T and w_y^T are linear combination coefficients, and X, Y are canonical variables, respectively. Now, we attempt to solve

$$\max_{\boldsymbol{w}_x,\boldsymbol{w}_y} \rho = \frac{C[X,Y]}{\sqrt{V[X]V[Y]}} \tag{3.2}$$

where C is covariance and V is variance. Without loss of generality we could assume a zero mean for both C and V. Therefore, the above expression can be written

$$\rho = \frac{E[XY]}{\sqrt{E[X^2]E[Y^2]}}$$

$$= \frac{E[\boldsymbol{w}_x{}^T \boldsymbol{x}\boldsymbol{y}^T \boldsymbol{w}_y]}{\sqrt{E[\boldsymbol{w}_x{}^T \boldsymbol{x}\boldsymbol{x}^T w_x]E[\boldsymbol{w}_y{}^T \boldsymbol{y}\boldsymbol{y}^T \boldsymbol{w}_y]}}$$

$$= \frac{\boldsymbol{w}_x{}^T \boldsymbol{C}_{xy} \boldsymbol{w}_y}{\sqrt{\boldsymbol{w}_x{}^T \boldsymbol{C}_{xx} \boldsymbol{w}_x \boldsymbol{w}_y{}^T \boldsymbol{C}_{yy} \boldsymbol{w}_y}} \tag{3.3}$$

where Cxx, Cxy, and Cyy are the covariance matrices. Therefore, the maximum ρ with respect to wx and wy is the maximum canonical correlation.

Assume $\sum_{xx} = cov(x, x)$, $\sum_{yy} = cov(y, y)$, a = wx , b = wy ,

$$\rho = \frac{a^T \sum_{xy} b}{\sqrt{a^T \sum_{xx} a \; b^T \sum_{yy} b}}$$

Now, the question is equal to maximize the $a^T \sum_{xy} b$ subject to

$$a^T \sum_{xx} a = 1 \; and \; b^T \sum_{yy} b = 1 \, ,$$

applying Lagrange multiplier:

$$\max \mathrm{L} = a^T \sum_{xy} b + \lambda_x \left[a^T \sum_{xx} b\right] + \lambda_y \left[a^T \sum_{xx} b\right] ,$$

applying partial derivative:

$$\rightarrow \begin{cases} \dfrac{\partial L}{\partial a} = \sum_{xy} b + 2\lambda_x \sum_{xx} a = 0 \\ \dfrac{\partial L}{\partial b} = \sum_{xy}^{T} a + 2\lambda_y \sum_{yy} b = 0 \end{cases}$$

$$\rightarrow \begin{cases} a^T \sum_{xy} b + 2\lambda_x \, a^T \sum_{xx} a = 0 \\ b^T \sum_{xy}^{T} a + 2\lambda_y \, b^T \sum_{yy} b = 0 \end{cases}$$

$$\rightarrow \begin{cases} a^T \sum_{xy} b = -2\lambda_x \\ b^T \sum_{xy}^{T} a = -2\lambda_y \end{cases}$$

$$\rightarrow \begin{cases} \sum_{xy} b = -2\lambda_x \sum_{xx} a \\ \sum_{xy}^{T} a = -2\lambda_y \sum_{yy} b \end{cases}$$

multiply $\sum_{yx} \sum_{xx}^{-1} \; and \; \sum_{xy} \sum_{yy}^{-1}$ respectively:

$$\rightarrow \begin{cases} \sum_{yx} \sum_{xx}^{-1} \sum_{xy} b = -2\lambda_x \sum_{xy}^{T} a \\ \sum_{xy} \sum_{yy}^{-1} \sum_{xy}^{T} a = -2\lambda_y \sum_{xy} b \end{cases}$$

since $\sum_{xy}^{T} a = \sum_{xy} a$,

$$\rightarrow \begin{cases} \sum_{yx} \sum_{xx}^{-1} \sum_{xy} b = -2\lambda_x \sum_{xy}^{T} a \\ \sum_{xy} \sum_{yy}^{-1} \sum_{yx} a = -2\lambda_y \sum_{xy} b \end{cases}$$

$$\rightarrow \begin{cases} \sum_{yx} \sum_{xx}^{-1} \sum_{xy} b = 4\lambda_x^2 \sum_{yy} b \\ \sum_{xy} \sum_{yy}^{-1} \sum_{yx} a = 4\lambda_y^2 \sum_{xx} a \end{cases}$$

therefore, the canonical correlations can be found by solving the following eigenvalue equations:

$$\begin{cases} \sum_{yy}^{-1} \sum_{yx} \sum_{xx}^{-1} \sum_{xy} b = 4\lambda_x^2 \, b = \rho^2 \, b \\ \sum_{xx}^{-1} \sum_{xy} \sum_{yy}^{-1} \sum_{yx} a = 4\lambda_y^2 \, a = \rho^2 \, a \end{cases}$$

More detail usage can be found in [44]. Several studies have proposed applying this approach in EEG data [5][14]. In the SSVEP-based BCI application, the source data sets (x) consisted of SSVEPs and the reference data set (y) consisted of sinusoidal and cosine with second harmonic signals. The reference data set used the fundamental stimulus frequency plus the second harmonic frequency as follows:

$$\text{y(t)} = \begin{pmatrix} sin(2\pi ft) \\ cos(2\pi ft) \\ sin(4\pi ft) \\ cos(4\pi ft) \end{pmatrix}, \text{t} = \frac{1}{SR}, \frac{2}{SR}, \ldots \frac{N}{SR}$$

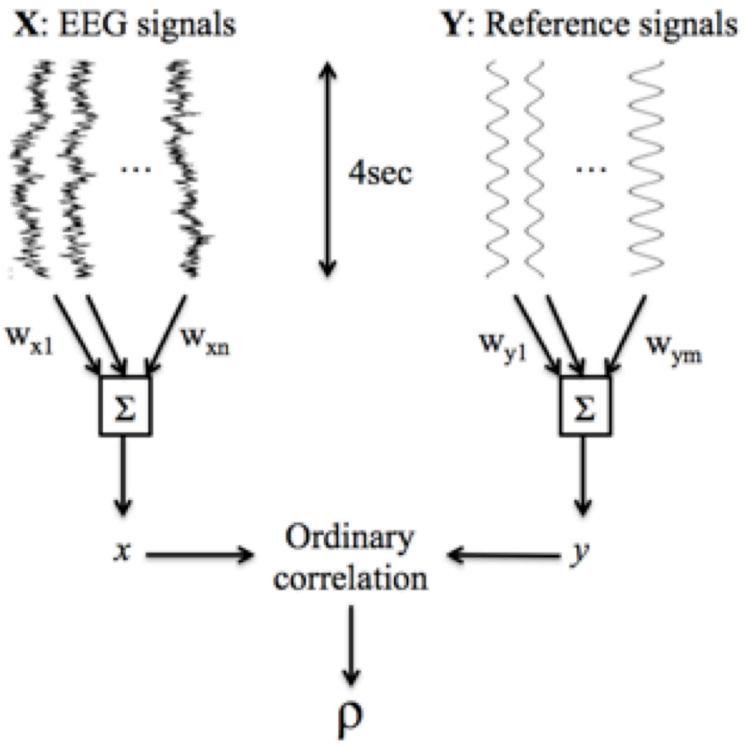

Figure 3.2 An graphic illustration of the CCA algorithm. Note that the *x* and *y* are projected vectors on specific basis that can contribute maximum correlation.

where f is the stimulus frequency, SR is sampling rate and N is the number of data points. Note that, the third or higher harmonic frequency might not improve the performance [14].

Figure 3.2 also graphically shows the basic CCA usage. CCA acts similar to a special filter that translates the multi-dimension data into one dimension, such that the projected X and Y are form one dimensional dataset with maximum correlation.

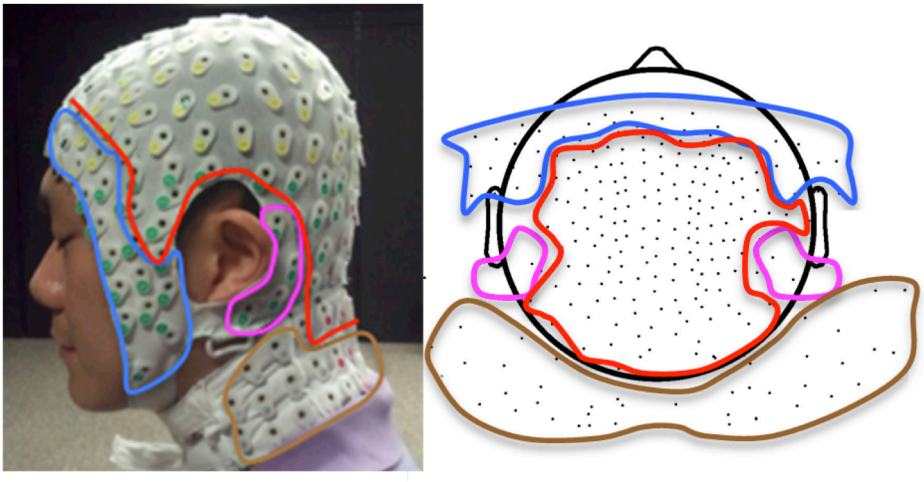

(a) (b)

Figure 3.3 Electrode placement for the hair-covered and non-hair-bearing areas. (a) A subject wore a 256-channel electrode cap. The red line roughly delineates the boundaries between the hair and non-hair-bearing areas of the subject. Blue, magenta and brown circles represent the electrodes locate at the forehead/face, behind-the-ear, and neck areas, respectively. (b) Top view of the distribution of the scalp electrodes.

In this section, we addressed the definition of noise, artifact, fundamental signals, and SNR. Moreover, some useful methods of manipulating signals were also presented. It is not easy to find a method that can apply to every application such that the performance is significantly improved. One should consider the purpose and hardware resource to choose an optimal algorithm.

3.3.1 SINGLE-CHANNEL EVALUATION

Since this study aims to investigate the SNR of SSVEPs recorded from non-hear-bearing areas, the SNR values for all electrodes were calculated, sorted, and categorized into four areas as indicated in Figure 3.3 In each of the four areas, the electrode with the highest SNR was selected for comparison. In the hair-covered area

delineated by the red line, the electrode with the highest SNR was located in the occipital region. This procedure was applied to all stimulus frequencies.

3.3.2 MULTI-CHANNEL EVALUATION

The spatial filtering technique has been widely used in EEG signal processing to improve the SNR of the EEG signals recorded from multiple scalp locations. In previous studies of SSVEP-based BCIs, the CCA algorithm has proved to be very efficient for improving the SNR of SSVEP signal [14]. CCA can calculate the canonical coefficients for the two different datasets (in this case, EEG dataset and a reference signal set) such that the correlation between the two canonical variables was maximized. The reference signal set is defined as

$$\begin{Bmatrix} \sin(2\pi ft) \\ \cos(2\pi ft) \end{Bmatrix} \tag{3.2}$$

where f is the stimulating frequency. In practice, the coefficients for the EEG dataset could be used as spatial filters to compute linear combinations of EEG data from all electrodes. For multi-channel data, the SNR of SSVEPs was calculated using the projection of the multi-channel data (i.e., the canonical variable).

The SNR of the multi-channel data was estimated by calculating the mean SNR of randomly selected combinations of electrodes from the 80 electrodes over the non-hair-bearing areas. The number of selected electrodes ranged from 1 to 80. For each number, the SNR calculation was repeated 1,000 times with different electrode combinations. The SNR and electrode positions of the combination with the highest SNR were saved for further comparison.

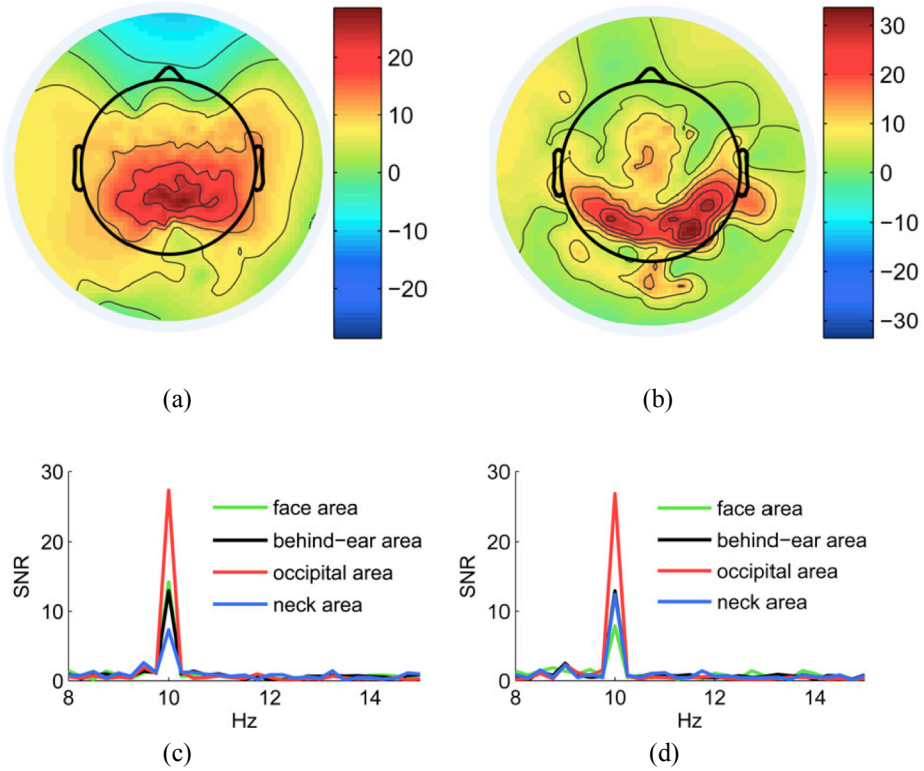

Figure 3.4 Scalp topography of the SNR's of SSVEPs at 10 Hz for (a) Subject 1, (b) Subject 5. Single-channel SNR from the occipital and non-hair-bearing areas for (c) Subject 1, (d) Subject 5.

3.4 RESULTS

Figure 3.4 shows the SNR topography and the normalized amplitude spectrum on different head areas for Subject 1 and Subject 5. As expected, the occipital area has the highest SNR of SSVEP signals, indicating that the brain sources might locate in or near the visual cortex. The SNR depended on the distance between the electrode position and the occipital region. As shown in Figure 3.4 (a) and (b), the SNR decreased at other brain areas (e.g., the frontal area) and non-hair-bearing areas. Although the SNR of SSVEP signals recorded from the non-hair-bearing areas was

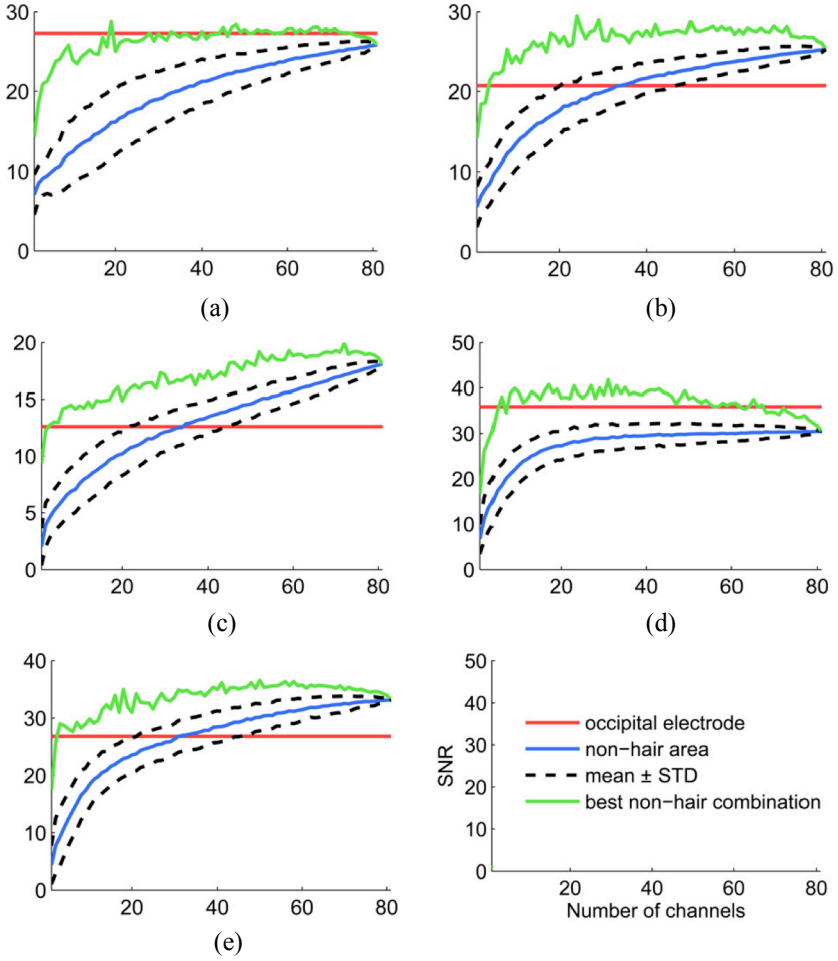

Figure 3.5 The relationship between the SNR and the number of electrodes used in the CCA processing. (a) - (e) correspond to Subject 1-5, respectively. The non-hair-bearing electrodes include those from the face, neck, and behind-the-ear areas. The signals measured from the occipital electrodes had the highest SNR.

lower than that recorded from the occipital region, signals acquired from the non-hair-bearing areas still showed a clear frequency response at the stimulating frequency (see Figure 3.4 (c) and (d)). This finding confirmed our hypothesis that the SSVEPs might be detectable from EEG signals measured from the non-hair-bearing areas on the head.

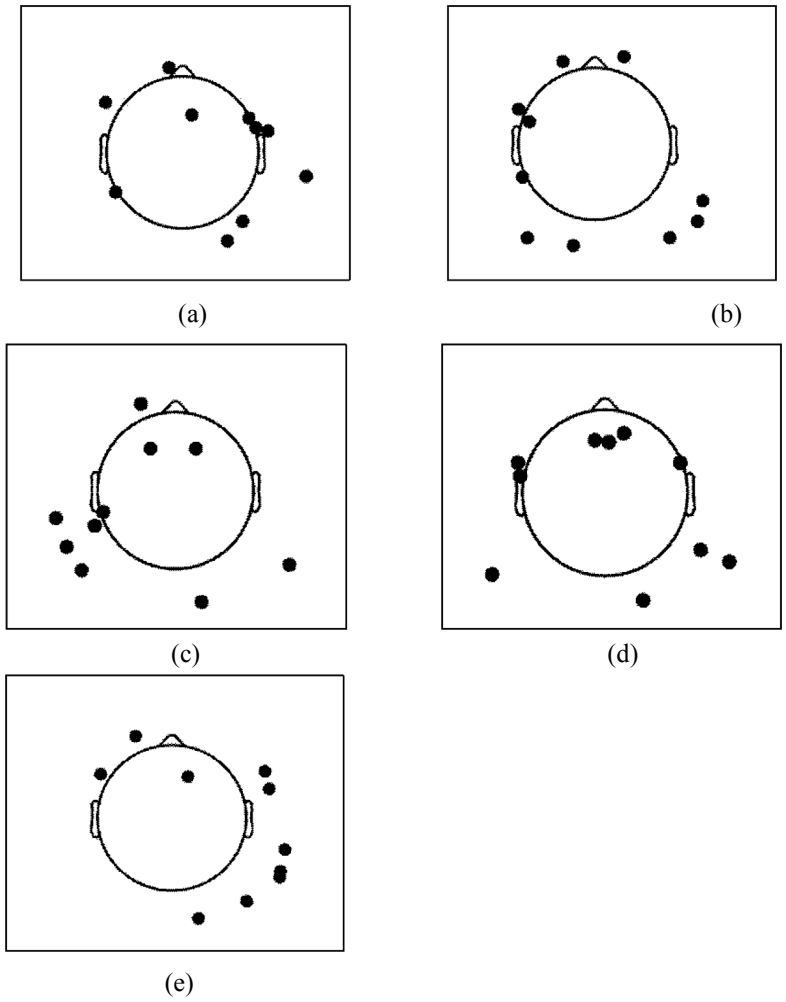

Figure 3.6 The 2-D projection for the placement of 10 electrodes that result in the highest SNR for each of the 5 subjects. (a) - (e) correspond to Subjects 1-5, respectively. The black dots indicate the electrode locations over the non-hair areas.

Figure 3.5 illustrates the SNRs of SSVEP signals contributed by combinations of data from multiple electrodes placed at the non-hair-bearing areas for all subjects. For a single electrode, the occipital electrode has a much higher SNR than any electrode from the non-hair-bearing areas. In general, the SNR increased as the number of electrodes involved in the CCA processing increased (as indicated by the blue solid line in Figure 3.5). For all the subjects, the best combination of multiple electrodes

from the non-hair-bearing areas reached an SNR comparable to the occipital electrode. In particular, three subjects (Subjects 2, 3 and 5) had SNRs of non-hair SSVEPs even higher than those of the occipital electrode. All subjects reached comparable SNRs by using the optimal occipital electrode and a combination of 10 non-hair-bearing electrodes. For Subjects 2, 3, and 5, using as few as five non-hair-bearing electrodes could exceed the SNR of the occipital electrode.

Next, this study explores the optimal placements of multi-channel non-hair-bearing electrodes to realize a practical SSVEP-based BCI system. Figure 3.6 shows the electrode placements with the highest SNR using 10 electrodes. For all the subjects, the 10 optimal electrodes covered multiple non-hair-bearing areas, all contributing to the improvement of the SNR of SSVEPs. This individualized electrode montage has the potential to result in many practical BCI applications.

3.5 CONCLUSION

SSVEP-based BCI applications have attracted a lot of attention recently. However, to our best knowledge, no study has systematically compared the SNR of SSVEPs measured from hair-covered and non-hair-bearing areas. This study showed that, across the five subjects, EEG recordings from non-hair-bearing areas, including the face, neck, and behind the ear areas, could reliably measure SSVEPs. Generally speaking, the rank of the SNR was the occipital area > behind-the-ear > neck area ≈ face area. A lower SSVEP SNR obtained from the neck and face areas might be attributed to the contamination from the muscle activity to those areas.

The comparison between hair-covered and non-hair-bearing area showed that the quality of SNR depends on the electrodes selections. As shown in Figure 3.3, the SNR of non-hair-bearing SSVEPs of Subject 3 matched well with that of the reference channel by using only two electrodes. The comparable results were found in Subjects 2 and 5. These results suggested that, if an optimal non-hair electrode combination could be known in advance, one could achieve comparable SNRs of SSVEP by using electrodes placed on the non-hair-bearing areas and the occipital area.

Using laboratory-oriented EEG setups for real-world SSVEP BCI applications is known to be impractical for routine use. An alternative approach to obtain informative EEG signals over no-hair-bearing sites is thus highly desirable. The results of this study demonstrated the feasibility of using a non-hair-bearing montage for measuring SSVEP, which we believe might significantly improve the practicality of BCI systems in real-life environments. If the proposed apparatus proves feasible in other BCI practices, a much wider range of applications of BCI will emerge.

ACKNOWLEDGMENTS

This chapter contains material from “Measuring Steady-State Visual Evoked Potentials from non-hair-bearing areas” by Yu-Te Wang, Yijun Wang, Chung-Kuan Cheng, and Tzyy-Ping Jung, which appears in the *34th Annual International Conference of the IEEE Engineering in Medicine and Biology Society (IEEE EMBC 2012)*. The dissertation author was the first investigator and author of this paper.

Chapter 4

A Cell-Phone Based Brain-Computer Interface for Communication in Daily Life

Moving a brain-computer interface (BCI) system from a laboratory demonstration to real-life applications still poses severe challenges to the BCI community. This study aims to integrate a mobile and wireless electroencephalogram (EEG) system and a signal-processing platform based on a smartphone into a truly wearable and wireless online BCI. Its practicality and implications in routine BCI are demonstrated through the realization and testing of a steady-state visual evoked potential (SSVEP)-based BCI. This study implemented and tested online signal processing methods in both time and frequency domains for detecting SSVEPs. The results of this study showed that the performance of the proposed smartphone based platform was comparable, in terms of information transfer rate (ITR), with other BCI systems using bulky commercial EEG systems and personal computers. To the best of our knowledge, this study is the first to demonstrate a truly portable, cost-effective, and miniature smartphone based platform for online BCIs

4.1 BACKGROUND

Brain-computer interface (BCI) systems acquire electroencephalography (EEG) signals from the human brain and translate them into digital commands, which can be recognized and processed on a computer or computers using advanced algorithms [1]. It can also provide a new interface for the users who have motor disabilities to control assistive devices such as wheelchairs.

Although EEG-based BCIs have already been studied for several decades, moving a BCI system from a laboratory demonstration to real-life applications still poses severe challenges to the BCI community [22]. To design a practical BCI system, the following issues need to be addressed [12][27][45]: (1) ease of use, (2) robustness of system performance, and (3) low-cost hardware and software. In real-life applications, BCI systems should not use bulky, expensive, wired EEG acquisition device and signal processing platforms [20]. Using these devices will not only cause discomfort and inconvenience for the users, but also affect their ability to perform routine tasks in real life. Recently, with advances in the biomedical sciences and electronic technologies, the development of a mobile and online BCI has been put on the agenda [19].

Several studies have demonstrated the use of portable devices for BCIs [13] [19][20]. Lin et al. [20] proposed a portable BCI system that can acquire and analyze EEG signals with a custom DSP module for real-time cognitive-state monitoring. Shyu et al. [13] proposed a system to combine an EEG acquisition circuit with an FPGA-based real-time signal processer. Recently, with the advances in integrated

circuit technology, smartphones combined with DSP [21] and built-in Bluetooth function have become very popular in the consumer market. Compared with the PC-based or customized platforms, the ubiquity, mobility, and processing power of smartphones make them a potentially vital tool in creating on-line and portable BCIs that need real-time data transmission, signal processing, and feedback presentation in real-world environments.

Although the EEG-based BCI technology using PCs and the Bluetooth transmission of bio-signals have been well established in previous studies, the feasibility of a portable smartphone based BCI, which supports biomedical signal acquisition and on-line signal processing, has never been explored. This portable system emphasizes usability "on-the-go", and the freedom that smartphones enable. If a smartphone based BCI proves to be feasible, many current BCI demonstrations (e.g. gaming, text messaging, etc.) can be realized on smartphones in practice and numerous new applications might emerge. This study integrates a portable, wireless, low-cost EEG system and a smartphone based signal processing platform into a truly wearable online BCI. The system consists of a four-channel bio-signal acquisition/amplification module, a wireless transmission module, and a Bluetooth-enabled smartphone. The goals of this study are to demonstrate the practicality of the proposed system by specifically answering the following questions: (1) is the quality of the EEG data collected by the custom wireless data acquisition device adequate for the routine BCI use? (2) is it feasible to implement time- and/or frequency-domain signal-processing algorithms (e.g., EEG power spectrum estimation and EEG spatial

filtering approaches) on a regular smartphone in real time?

To address these technical issues, a steady-state visual evoked potential (SSVEP)- based BCI, which has recognized advantages of ease of use, little user training and high information transfer rate (ITR) was employed as a test paradigm. SSVEP is the electrical response of the brain to the flickering visual stimulus at a repetition rate higher than 6 Hz [4], which is characterized by an increase in amplitude at the stimulus frequency. We adopted the widely used frequency-coding approach to build an online BCI on a smartphone. In SSVEP BCI, the attended frequency-coded targets of the user are recognized through detecting the dominant frequency of the SSVEP. To this end, several signal-processing methods have been proposed and demonstrated [46]. Among them, power spectrum density (PSD) estimation (e.g., Fast Fourier Transform (FFT)) is most widely used in online SSVEP BCIs [27][30][46]. Recently, a Canonical Correlation Analysis (CCA) method was proposed and implemented in an online multi-channel SSVEP BCI, achieving an ITR of 58 bits/min [14]. To explore the plausibility of an on-line smartphone based BCI platform, this study implemented and tested both single-channel FFT and multi-channel CCA methods for processing SSVEPs induced by attended targets.

4.2 Method

In this Section, we address the BCI system in terms of the hardware and software architecture.

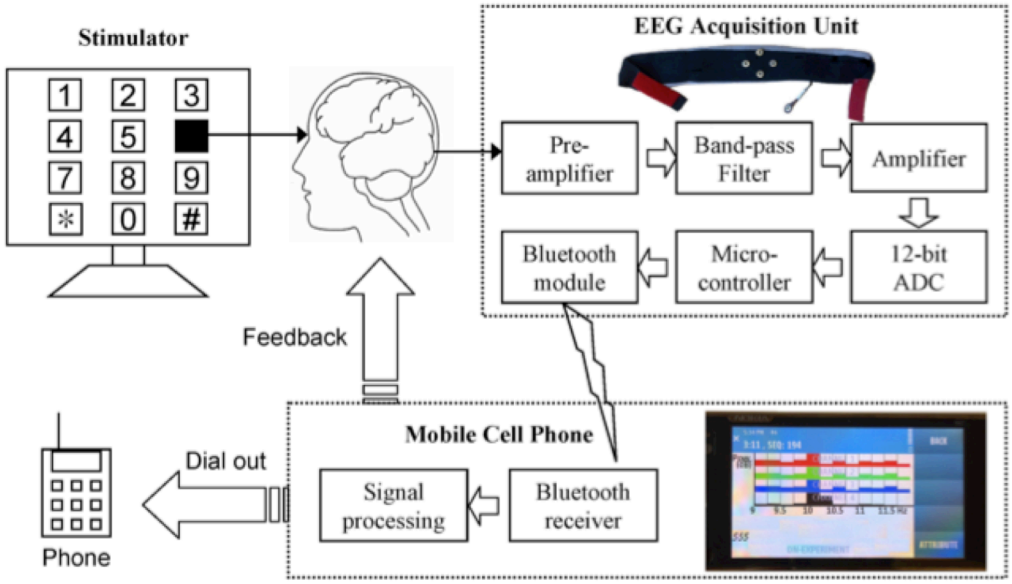

Figure 4.1 The system diagram of the mobile and wireless BCI system.

4.2.1 SYSTEM HARDWARE DIAGRAM

A typical VEP-based BCI using frequency coding consists of three parts: a visual stimulator, an EEG recording device and a signal-processing unit [46]. Figure 4.1 depicts the basic scheme of the proposed mobile and wireless BCI system. This study adapts a mobile and wireless EEG headband from [19] as the EEG recording device and a Bluetooth-enabled smartphone as a signal-processing platform.

The visual stimulator comprises a 21-inch CRT monitor (140Hz refresh rate, 800x600 screen resolution) with a 4 x 3 stimulus matrix constituting a virtual telephone keypad that includes digits 0-9, BACKSPACE and ENTER. The stimulus frequencies ranged from 9Hz to 11.75Hz with an interval of 0.25Hz between two consecutive digits. In general, this cannot be implemented with a fixed rate of black/white flickering pattern due to a limited refresh rate of a LCD screen. Wang et al [8] recently

developed a new method that approximates target frequencies of SSVEP BCI with variable black/white reversing intervals. For example, presenting an 11Hz target stimulus on a screen refreshed at 60-Hz can be realized with 11-cycle black/white alternating patterns lasting [3 3 3 2 3 3 3 2 3 3 2 3 3 3 2 3 3 3 2 3 3 2] frames in a second. Based on this approach, any stimulus frequency up to half of the refresh rate of the screen can be realized. The stimulus program was developed in Microsoft Visual C++ using the Microsoft DirectX 9.0 framework.

The EEG acquisition unit is a 4-channel, wearable bio-signal acquisition unit [45]. EEG signals were amplified (8,000x) by instrumentation amplifiers, Band-pass filtered (0.01-50 Hz), and digitized by analog-to-digital converters (ADC) with a 12-bit resolution. To reduce the number of wires for high-density recordings, the power, clocks and measured signals were daisy-chained from one node to another with bit-serial outputs. That is, adjacent nodes (electrodes) are connected together to (1) share the power, reference voltage, and ADC clocks and (2) daisy chain the digital outputs. Next, TI MSP430 was used as a controller to digitize EEG signals using ADC via serial peripheral interface with a sampling rate of 128Hz. The digitized EEG signals were then transmitted to a data receiver such as a smartphone via a Bluetooth module. In this study, Bluetooth module BM0203 was used. The whole circuit was integrated into a light-weight headband.

4.2.2 SYSTEM SOFTWARE DESIGN

The signal-processing unit was realized using a Nokia N97 (Nokia Inc.) smartphone. A J2ME program developed in Borland JBuilder2005 and Wireless

Development Kit 2.2 were installed to perform online procedures including (1) displaying EEG signals in time-domain, frequency-domain and CCA-domain on the LCD screen of the smartphone, (2) band-pass filtering, (3) estimating the dominant frequencies of the VEP using FFT or CCA, (4) delivering auditory feedback to the user and (5) dialing a phone call. The resolution of the 3.5-in touch screen of the phone is 640 x 360 pixels.

When the program is launched, the connection to the EEG acquisition unit would be automatically established in just a few seconds. The EEG raw data are transferred, plotted and updated every second on the screen. Since the sampling rate is 128 Hz, the screen displays about 4-second of data at any given time. Users can choose the format of the display between time-domain and frequency-domain. Under the frequency-domain display mode, the power spectral densities of 4-channel EEG will be plotted on the screen and updated every second. An auditory and visual feedback would be presented to the user once the dominant frequency of the SSVEP is detected by the program. For example, when number 1 is detected by the system, the digit "1" would be shown at the bottom of the screen and "ONE" would be said at the same time.

Software operation and user interface include several functions. First, the program initiates a connection to the EEG acquisition unit. Second, four-channels of raw EEG data are band-pass filtered at 8-20 Hz, and then plotted on the screen every second. Third, the display can be switched to the power spectrum display or time-domain display by pressing a button at any time. Figure 4. 1 includes a screen shot of the smartphone, which plots the EEG power across frequency bins of interest. Fourth,

an FFT or CCA mode can be selected. In the FFT mode, a 512-point FFT is applied to the EEG data using a 4-second moving window advancing at 1-second steps for each channel. In the CCA mode, it uses all four channels of the EEG with a 2-second moving window advancing at 1-second steps continuously. The maximum window length is 8 second. Detailed procedures and parameters of the CCA method can be found in [14]. To improve the reliability, a target is detected only when the same dominant frequency is detected in two consecutive windows (at time k, and k+1 seconds, $k \geq 4$ in the FFT mode, and ≥ 2 in the CCA mode). The subjects were instructed to shift their gaze to the next target once they heard the auditory feedback.

4.3 BCI EXPERIMENT DESIGN

Ten volunteers with normal or corrected to normal vision participated in this experiment. All participants were asked to read and sign an informed consent form before participating in the study. The experiments were conducted in a typical office room without any electromagnetic shielding. Subjects were seated in a comfortable chair at a distance of about 60 cm to the screen. Four electrodes on the EEG headband were placed 2 cm apart, surrounding a midline occipital (Oz) site, all referred to a forehead midline electrode (the sensor array is shown in Figure 4. 1).

FFT and CCA based approaches were tested separately. All subjects participated in the experiments during which the smartphone used FFT to detect frequencies of SSVEPs, and four subjects were selected to do a comparison study between using FFT and CCA for SSVEP detection. At the beginning of experiment, each subject was asked to gaze at some specific digits to confirm the wireless

connection between the EEG headband and the smartphone. In the FFT mode, the channel with the highest signal-to-noise ratio, which is based on the power spectra of the EEG data, was selected for online target (digit) detection. Four of 10 subjects who have better performance (i.e. higher ITR in the FFT mode) were selected to further test the CCA-based SSVEP BCI. The test session began after a couple of short practice sessions. The task was to input a 10-digit phone number: 123 456 7890, followed by an ENTER key to dial the number. Incorrect key detection could be erased by attending to the "BACKSPACE" key. In the CCA mode, the same task was repeated six times, leading to 11x6 selections for each subject. The EEG in the CCA experiments were saved with feedback codes for an offline comparison study between FFT and CCA. The percentage accuracy and ITR [1] were used to evaluate the BCI performance.

4.4 RESULTS

Tables 4.1 and 4.2 show results of SSVEP BCI using FFT and CCA, respectively. In the FFT mode, all subjects completed the phone-dialing task with an average accuracy of 95.9±7.4%, and an average time of 88.9 seconds. Seven of 10 subjects successfully inputted 11 targets without any errors. The average ITR was

Table 4.1 FFT-based online test results of SSVEP BCI in 10 subjects.

Subject	Input length	Time (second)	Accuracy (%)	ITR (bits/min)
s1	11	72	100	32.86
s2	11	72	100	32.86
s3	19	164	78.9	14.67
s4	11	73	100	32.4
s5	17	131	82.4	17.6
s6	11	67	100	35.31
s7	11	72	100	32.86
s8	13	93	92.3	20.41
s9	11	79	100	29.95
s10	11	66	100	35.85
Mean	12.6	88.9	95.9	28.47

Table 4.2 CCA-based test results (ITR) of SSVEP BCI in four subjects.

Subject	Online CCA	Online FFT	Offline FFT	**Putative** ITR from off-line FFT			
				Ch1	Ch2	Ch3	Ch4
1	44.79	32.86	36.68	**36.68**	33.58	32.48	29.77
2	46.25	32.86	26.49	**26.49**	10.51	5.91	9.29
6	49.05	35.31	19.43	**19.43**	3.03	3.15	1.92
10	43.18	35.85	15.24	2.2	8.46	**15.24**	4.21
Mean	45.82	34.22	24.46	21.2	13.9	14.2	11.3

28.47±7.8 bits/min, which was comparable to other VEP BCIs implemented on a high-end personal computer [27]. Table 2 shows the results of SSVEP BCI using online CCA on the smartphone. CCA achieved an averaged ITR of 45.82±2.49 bits/min, which is higher than that of the FFT-based online BCI of the four participants (34.22 bits/min). Applying FFT to the EEG data recorded during the experiments using the online CCA resulted in an averaged putative ITR of 24.46 bits/min, using the channel with the highest accuracy for each subject (cf. right columns of Table 4.2).

4.5 CONCLUSIONS

This study designed, developed and evaluated a portable, cost-effective, and miniature smartphone based online BCI platform for communication in daily life. A mobile, lightweight, wireless and battery-powered EEG headband was used to acquire and transmit EEG data of unconstrained subjects in real-world environments. The

acquired EEG data were received by a regular smartphone through Bluetooth. Advances in mobile phone technology have allowed phones to become a convenient platform for real-time processing of the EEG. The smartphone based platform propels the mobility, convenience and usability of online BCIs.

The practicality and implications of the proposed BCI platform were demonstrated through the high accuracy and ITR of an online SSVEP-based BCI. To explore the capacity of the smartphone platform, two experiments were carried out using an online single-channel FFT and a multi-channel CCA algorithm. The mean ITR of the CCA mode was higher than that of the FFT approach (~45 bits/min vs. 34 bits/min) in the four participants. An off-line analysis, which applied FFT to the EEG data recorded during the online CCA-based BCI experiments, showed the target selection was less accurate using FFT than CCA, which in turn resulted in a lower ITR (Table 2). The decline in accuracy and ITR in offline FFT analysis could be attributed to a lack of sufficient data for FFT to obtain accurate results. In other words, FFT, in general, required more data (longer window) than CCA to accurately estimate the dominant frequencies in SSVEPs (6 seconds vs. 4 seconds). Further, the multi-channel CCA approach eliminated the need for manually selecting the 'best' channel prior to FFT analysis.

Despite this successful demonstration of a smartphone based BCI, there is room for improvement. Future directions include: (1) the use of dry EEG electrodes over the scalp locations covered with hairs to avoid skin preparation and the use of conductive gels; and (2) the use of higher-density EEG signals to enhance the

performance of the BCI [17]. However, high-density EEG might increase the computational need in BCIs. With advances in smartphone technology, more powerful onboard processors can be expected in a foreseeable future, enabling the implementation of more sophisticated algorithms for online EEG processing.

Notably, in the current study, the smartphone was programmed to assess wearer's SSVEPs for making a phone call, but it can actually be programmed to realize other BCI applications. For example, the current system can be easily converted to realize a motor imagery based BCI through detecting EEG power perturbation of mu/beta rhythms over the sensorimotor areas. In essence, this study is just a demonstration of a smartphone based platform technology that can enable and/or facilitate numerous BCI applications in real-world environments.

ACKNOWLEDGMENTS

This chapter is reprinted from "A Smartphone Based Brain-Computer Interface for Communication in Daily Life" by Yu-Te Wang, Yijun Wang, and Tzyy-Ping Jung, which appears in the *Journal Of Neural Engineering* Vol.8, No.2, 2011. The dissertation author was the first investigator and author of this paper.

Chapter 5

Developing an EEG-based On-line Closed-loop Lapse Detection and Mitigation System

In America, sixty percent of adults reported that they have driven a motor vehicle while feeling drowsy, and at least 15-20% of fatal car accidents are fatigue-related. This study translates previous laboratory-oriented neurophysiological research to design, develop, and test an On-line Closed-loop Lapse Detection and Mitigation (OCLDM) System featuring a mobile wireless dry-sensor EEG headgear and a smartphone based real-time EEG processing platform. Eleven subjects participated in an event-related lane-keeping task, in which they were instructed to manipulate a randomly deviated, fixed-speed cruising car on a 4-lane highway. This was simulated in a 1st person view with an 8-screen and 8-projector immersive virtual-realty environment. When the subjects experienced lapses or failed to respond to events during the experiment, auditory warning was delivered to rectify the performance decrements. However, the arousing auditory signals were not always effective. The EEG spectra exhibited statistically significant differences between effective and

ineffective arousing signals, suggesting that EEG spectra could be used as a countermeasure of the efficacy of arousing signals. In this on-line pilot study, the proposed OCLDM System was able to continuously detect EEG signatures of fatigue, deliver arousing warning to subjects suffering momentary cognitive lapses, and assess the efficacy of the warning in near real-time to rectify cognitive lapses. The on-line testing results of the OCLDM System validated the efficacy of the arousing signals in improving subjects' response times to the subsequent lane-departure events. This study may lead to a practical on-line lapse detection and mitigation system in real-world environments.

5.1 BACKGROUND

Fatigue-related performance decrements such as lapses in attention and slowed reaction time could lead to catastrophic incidents in occupations ranging from ship navigators to airplane pilots, railroad engineers, truck and auto drivers, and nuclear plant monitors. Fatigue (or drowsiness) “concerns the inability or disinclination to continue an activity, generally because the activity has been going on for too long”, defined by European Transport Safety Council [47]. Sixty percent of American adults reported that they have been driving a motor vehicle when feeling drowsy [48]. Furthermore, studies have concluded that at least 15-20% of fatal car accidents are fatigue-related [47][49][50]. Therefore, an earlier detection of driving fatigue is a crucial issue for preventing catastrophic incidents.

In order to detect the driving fatigue, several approaches have been proposed in scientific literature. (1) Computer vision-based systems [51][52][53]. Bergasa et al. [51] used a real-time image-acquisition system to monitor drivers' visual behaviors that revealed a drivers' alertness level. Six parameters: percentage of eye closure, eye closure duration, blink frequency, nodding frequency, face position, and fixed gaze were included in a fuzzy classifier for identifying a driver's vigilance level. D'Orazio et al. [52] proposed a neural classifier to recognize the eye activities from images without being constrained to head rotation or partially occluded eyes. (2) Driving behavior counter-measurements [45][54][55]. Lin et al. [45] performed an event-related, lane-keeping driving task in an immersive virtual-reality environment. Subjects were asked to steer the stimulated car back to the middle of the cruising lane once they perceived the randomized lane-departure events. The results showed that the reaction time (RT), defined as the time interval between the onset of the simulated car deviation and the user response, could be improved by providing arousing auditory warning to the subjects combating with fatigue.

A Brain Computer Interface (BCI) translates neural activities into control signals to provide a direct communication pathway between the human brain and an external device [1]. Broadly speaking, BCIs can be grouped into three categories: active, passive and reactive BCIs [56]. Electroencephalogram (EEG)-based passive BCIs measure brain electrical activities from the scalp and enrich a human–machine interaction with implicit information on the actual user state without conscious effort from the user [56]-[59]. Given appropriate signal-processing algorithms in the passive

BCIs, meaningful information can be directly extracted from the EEGs. For instance, time-domain analysis such as averaging across different channels, moving average with a specific window length, standard deviation, linear correlation and so on are useful approaches to extract information from EEGs [60]. In a frequency-domain analysis, the short-time Fourier transform (STFT) is often applied to the EEG data to estimate the power spectral density in distinct frequency bands, including delta (1-3 Hz), theta (4-7 Hz), alpha (8-13 Hz), beta (14-30 Hz), and gamma (31-50 Hz). Many studies have shown that the brain dynamics linked to fatigue and behavioral lapses can be assessed by EEG power spectra [45][53][61]-[68], combinations of EEG band power [69], alpha spindle parameters [70] and autoregressive features [71]. These studies provided solid evidence for the neurophysiological correlates of fatigue and behavioral lapses. In short, while the physical- and behavioral symptom-based methods indirectly measure drivers' cognitive states, the neurophysiology-based methods offer a more direct path to assess the brain dynamic linked to fatigue and behavioral lapses with a high temporal resolution.

Efforts have also been made to assist individuals in combating fatigue and/or preventing lapses in concentration. For instance, Dingus et al. [72] and Spence and Driver [73] proposed using warning signals to maintain drivers' attention. The types of warning signals could be auditory [73], visual [74], tactile [75] or mixed [74]. Empirical results showed that auditory warning could reduce the number of lapses in sustained-attention tasks, and could help subjects to maintain driving performance [54] [73]. More recent studies demonstrated that arousing auditory signals presented to

individuals experiencing momentarily behavioral lapses could not only agitate their behavioral responses but also change their EEG theta and alpha power in a sustained-attention driving task [45][55][76]. However, the studies also showed that sometimes subjects did not respond to the arousing signals, and more importantly the EEG activity of these non-responsive episodes showed little or no changes following the ineffective warning [45][55][76]. Lin et al. [55] later demonstrated the feasibility of using the post-warning EEG power spectra to predict the (in)efficacy of the arousing warning. A caveat of their studies was that the arousing warning was delivered to subjects after they behaviorally failed to respond to lane-departure events. In reality, the delivery of arousing warning could have been too late because the behavioral lapse might have led to catastrophic consequences. A truly EEG-based lapse monitoring system needs to continuously and noninvasively observe EEG dynamics to predict fatigue-related lapses, deliver arousing signal to arouse the user, and assess the efficacy of the arousing signal to trigger a repeated or secondary warning signal if necessary. Furthermore, all of the aforementioned studies were conducted with traditional bulky and tethered EEG systems and were performed in well-controlled laboratories. However, it is argued that there might be fundamentally dynamic differences between laboratory-based and naturalistic human behavior in the brain [23]. It thus remains unclear how well the current laboratory-oriented knowledge of EEG correlates of cognitive-state changes can be translated into the highly dynamic real world.

This study aims to extend previous studies to design, develop and test a truly On-line Closed-loop Lapse Detection and Mitigation (OCLDM) System that can continuously monitor EEG dynamics, predict fatigue-related lapses based on EEG signals, arouse the fatigued users by delivering arousing signals, and assess the efficacy of the arousing signal based on EEG spectra. This study hypothesized that 1) EEG spectral values would differ under different arousal states; 2) it is feasible to predict lapses based on the spectral changes in the spontaneous EEG; 3) arousing warning delivered to cognitively challenged subjects would mitigate cognitive lapse, and 4) the rectified performance would be accompanied by the changes in EEG power spectra. This study conducted an off-line experiment to explore the neurophysiological correlates of lapses, which tested the abovementioned hypotheses and guided the development of a truly OCLDM system. The system was then validated by an on-line driving experiment. Furthermore, to be practical for routine use in a car or workplace by freely moving individuals, the EEG-based lapse monitoring system must be non-invasive, non-intrusive, lightweight, battery-powered, and easily to put on and take off [20]. This study thus also investigates the feasibility of using a practical, low-density, lightweight dry EEG headgear and a smartphone-based EEG-processing platform to build a truly mobile and wireless OCLDM System for real-life applications [77].

5.2 MATERIALS AND METHODS

This Section describes the design and implementation of the off-line and on-line driving experiments. Note that this study first explored the neurological responses

from the off-line recording, and then applied the results to the on-line driving experiment.

5.2.1 SUBJECTS

Eleven healthy and naive subjects (ten males and one female) with normal hearing and aged 20-28 years old participated in this study. All of them were free of neurological and psychological disorders. They were introduced how to manipulate the stimulated car and practiced ~10 min to get acquainted before the experiment started. None of them worked night shifts or traveled across multiple time zones in the previous two months. All participants were asked to read and sign the informed consent form before participating in the studies. After the experiments, subjects were asked to complete the questionnaire for assessing their cognitive states during the experiments.

5.2.2 EXPERIMENTAL EQUIPMENT

Experiments of this study were conducted in an 8-screen and 8-projector immersive virtual-realty (VR) environment that simulates the 1st person view scene of highway driving. This study adapted an event-related lane-departure driving paradigm originally proposed by Huang et al. that allowed objective and quantitative measures of momentary event-related brain dynamics following lane-departure events and driving-performance fluctuations over longer periods [76]. The VR scenes simulated driving at a constant speed (at ~100 km/hr) on a highway with the simulated car

randomly drifting away from the center of the cruising lane to simulate driving on non-ideal road surfaces or with poor alignment [54]. The scene was updated according to the land-departure events and the subject's manipulation. The vehicle trajectory, user's input, and lane-departure events could be accurately logged and time-synchronized to the EEG recordings [20]. There were no traffic or distractive objects other than 4-lane roads and dark sky appeared in the VR while the simulated car was cruising on the highway.

Thirty-two channel EEG data were collected from participants by the NuAmp system (32-channels Quick-Cap, Compumedics Ltd., VIC, Australia). The electrodes were placed according to a modified international 10-20 system with a unipolar reference at the right earlobe. The EEG activities were recorded with 500 Hz sampling rate and 16-bit quantization level.

5.2.3 EXPERIMENTAL PARADIGM

Figure 5.1(a) shows the experimental paradigm of this study. The simulated car starts cruising at a fixed speed (~100km/hr) on the 3rd lane and drifting to either right or left with equal probability within 8-10 sec. Subjects were instructed to steer the simulated car back to the 3rd lane as soon as they noticed the lane drift. The simulated car keeps cruising on the right (or left) most lane if the subjects failed to respond to lane drift. The baseline period of each lane-departure epoch is defined as the 3 sec before the onset of a lane-drifting event. The empty circle in Figure 1(a) represents the unexpected lane-departure events marked as the "deviation onset". After the deviation

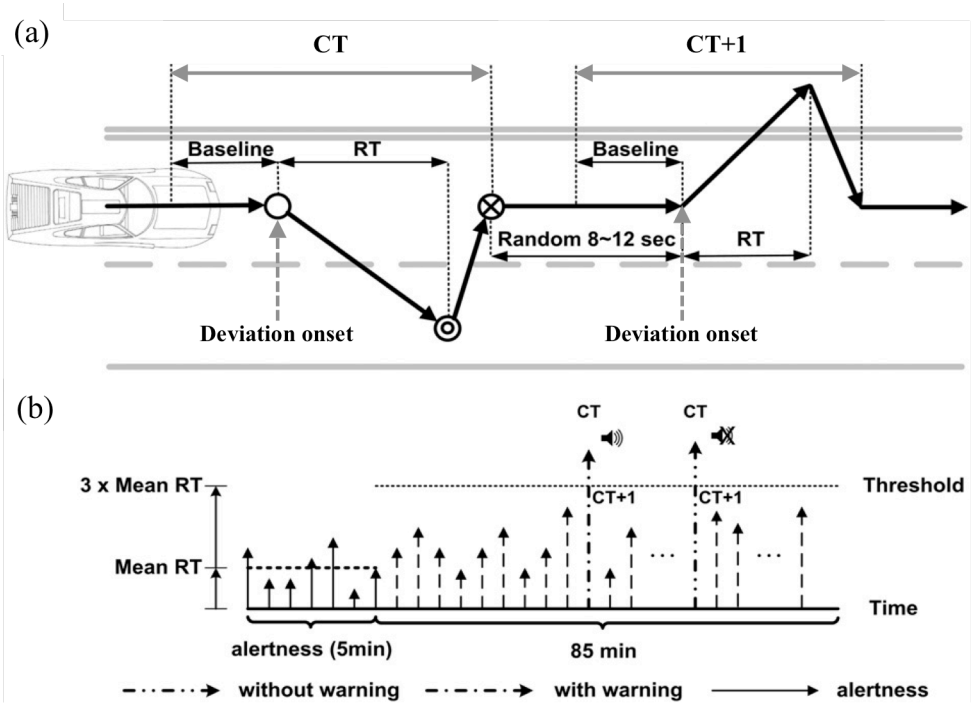

Figure 5.1 The off-line experiment paradigm. (a) Event-related lane-departure driving tasks. The solid arrows represent the driving trajectory. The empty circle represents the deviation onset. The double circle represents the response onset. The circle with the cross represents the response offset. The baseline is defined as the 3 sec period prior to deviation onset. The response time (RT) of a driver is the interval from the deviation (empty circle) to the response onset (the double circle). A trial starts at deviation onset and ends at response offset (circle with a cross). The next deviation begins 8-12 sec after response offset. (b) Criterion for delivering auditory warning during driving tasks. The height of an arrow represents the response time in a single trial. The warning was delivered to the subject when the RT in the trial exceeded three times the mean RT of trials in the first 5 min of the task, when the subject was presumably alert and fully attended to lane-departure events. This figure is adapted with permission from Fig. 1 of [45].

onset, subjects were instructed to steer the simulated car back to the center of the cruising lane immediately (double circle), and the time when the subjects started steering was marked as the "response onset". The moment that the simulated car reached the center of the cruising lane (circle with cross) was marked as the "response offset". A subject's response time (RT) was defined as the time between the deviation onset and the response onset. At the first 5 min of the experiment, subjects were asked

to be fully alert, verified by the vehicle trajectory and the video from a surveillance camera, to obtain an averaged alert RT (aRT) for each subject (1.51~2.54 sec), which is a threshold for the entire experiment. The entire experiment consisted of 5 min training and 85 min driving periods.

Figure 5.1(b) shows the criterion of delivering auditory warnings in the experiment. When a subject failed to respond within three times the aRT, the system treated the trials as a behavioral lapse and triggered a 1,750 Hz tone-burst to arouse the subject from fatigue-related lapse in half (50%) of these drowsy trials (marked as the "current trial (CT)" in Figure 5.1(a)). The very next trial is defined as CT+1, and so on. The lapse trials that were randomly selected to receive arousing warning were referred to as CT with warning, whereas the remaining half of trials that did not receive auditory warning were referred to as CT without warning. Note that our previous studies showed that in some trials subjects remained non-responsive following the arousing warning, which was analogous to sleeping through an alarm clock [55][76]. If the RT of the following trial (CT+1) was shorter than the double of the averaged aRT, the warning signal delivered in the CT trial was defined as an "effective warning". On the other hand, if the RT of the CT+1 trial was longer than triple of the averaged aRT, the warning was defined as an "ineffective warning". This study did not include the trials with RTs between 2-3 aRT to define the alert vs. fatigue spectral thresholds because the cognitive states of the subjects during those trials were unclear. Note that, subjects didn't know about the warning before the experiments.

5.2.4 DATA ANALYSIS

The 32-channel EEG data were first down-sampled to 250 Hz, and a low-pass filter of 50 Hz and a high-pass filter of 0.5 Hz were applied. Channels or trials with severe artifacts (such as body movements or muscle activities) were manually removed (less than three channels and 20% trials per subject in general). The remaining EEG data were segmented into several 115 sec trials, each of them consisting of 15 sec before and 100 sec after the lane-deviation onsets. Independent Component Analysis [40][41] implemented in EEGLAB [78] was then applied to decompose the ~32-channel EEG into ~32 independent components (ICs), based on the assumption that the collected EEG data from the scalp were a weighted linear mixture of electrical potentials projected instantaneously from temporally ICs accounting for distinct brain sources. The comparable ICs across subjects were grouped into component clusters based on their scalp maps, equivalent dipole locations and baseline power spectra of component activations [78][79]. Across 11 subjects, there were 155 trials with warning (30 trials were ineffective and 125 trials were effective) and 192 trials without warning.

Since the RT and EEG power were not normally distributed, nonparametric statistic tests were performed for the data analysis [78]. The Wilcoxon rank-sum test (Matlab statistical toolbox, Mathworks) was used to assess the effects of warning on RTs. Bootstrapping (EEGLAB toolbox, University of California, San Diego) was used to test the statistical significance of EEG power changes at specific frequency bins from 2 Hz to 30 Hz with a 0.25Hz resolution. To test group statistics, the intrinsic

inter-subject RT differences were reduced by dividing RTs by the mean RT. The EEG spectra were normalized by dividing the spectral power by the standard deviation of the spectral distribution.

5.3 NEUROPHYSIOLOGICAL CORRELATES OF BEHAVIORAL LAPSES

5.3.1. EFFICACY OF AROUSING AUDITORY SIGNALS FOR RECTIFYING LAPSES

This study first explored the efficacy of the delivery of arousing auditory signals by measuring the change in subjects' reaction time. Figure 5.2(a) shows the boxplots of RTs of three trial groups: Alertness, CT, and CT+1 (left to right). The averaged aRT of trials within the Alertness group across 11 subjects was ~676ms. The RTs of the CT group with arousing warning (red and light blue) were statistically significantly shorter than those of trials without receiving arousing warning (dark blue). The RTs of the CT+1 group with effective versus ineffective warning differed while the RTs of the preceding group (CT) were comparable. Even though the subjects responded to the arousing warning by immediately steering the simulated car back to the cruising position, they could well be totally non-responsive to the very next lane-departure event (~10 sec later). In other words, the arousing signals reliably rectified human behavioral lapses, but did not guarantee that subjects were fully awake, alert, or attentive. This suggests an analogous regime of snooze after an alarm is turned off.

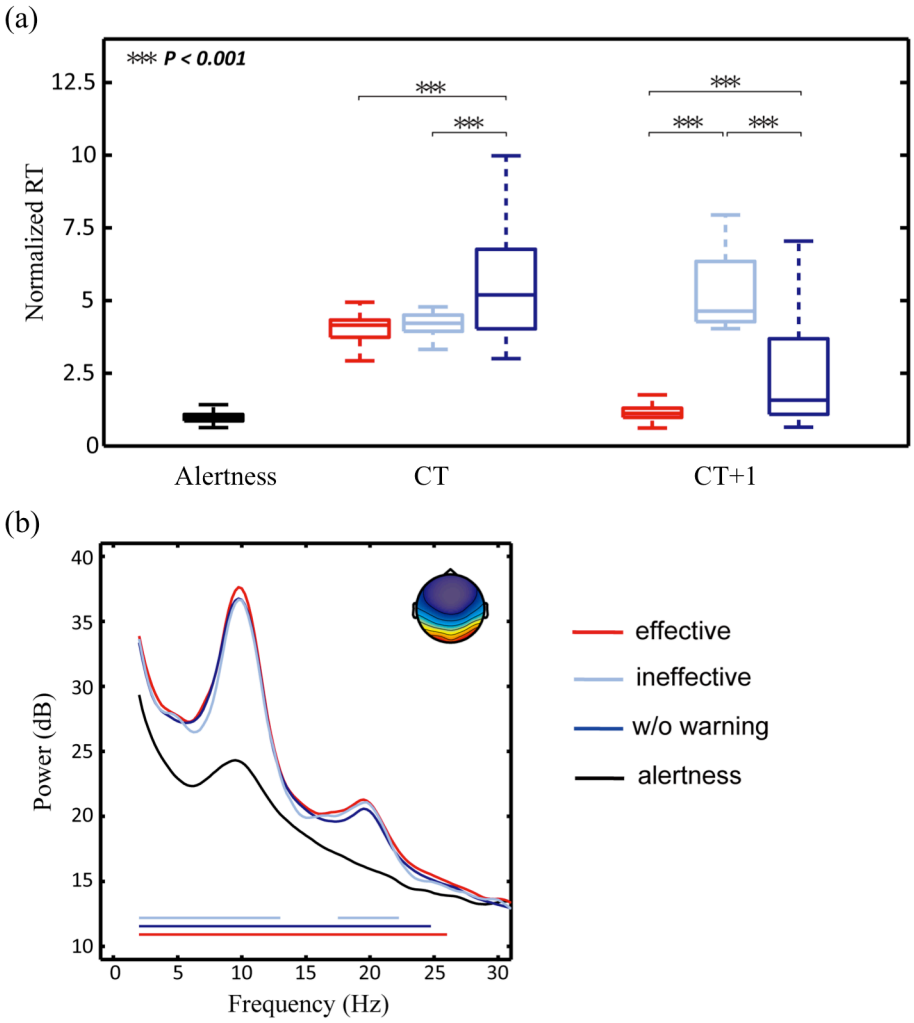

Figure 5.2 The off-line experiment results. (a) The boxplot for the RT distribution of trials with effective warning, ineffective warning, and without warning among CTs and CTs+1. Note that middle horizontal line is the median of the distribution, and the top and bottom of the rectangle are the third and first quartile, and the dash line ends are the maximum and minimum after outlier removal. (b) The component spectra of the alert CTs (black curve), with an effective warning (red curve), with an ineffective warning (light blue curve) and without warning (dark blue curve). The red, light blue and blue horizontal lines mark the spectral differences between the alert trials and trials with an effective warning, with an ineffective warning, and without warning, respectively. All the spectral plots were calculated from the activity of the bilateral occipital components separated by ICA.

5.3.2 EEG DYNAMICS PRECEDING BEHAVIORAL LAPSES

Figure 5.2(b) shows the mean scalp map of the bilateral occipital cluster (upper-right corner) and its component baseline power of drowsy trials without auditory warning (dark blue), with either effective (red) or ineffective warning (light blue). First, among the resultant ICA clusters, bilateral occipital components exhibited statistically significant spectral differences between trials with and without auditory warning. Second, the component power spectra exhibited tonic increases in theta (4-7 Hz), alpha (8-12 Hz), and beta (13-30 Hz) bands in drowsy trials (red, dark blue, and light blue), compared to the alert trials (black). Horizontal lines mark the frequency bins under which the spectral differences between alert trials and drowsy trials with either (in)effective warning, or without warning were statistically significant (alpha = 0.05, Bonferroni adjusted p value of 0.05/(112 frequency bins) = 0.0004 for multiple comparisons). Note that the spectra shown here were calculated from the component activities prior to the lane-deviation onset. The nearly identical pre-lapse spectra of these three groups of non-responsive trials demonstrate the robustness of the broadband spectral augmentation preceding the behavioral lapses, suggesting the feasibility of using theta and alpha power from the lateral occipital areas to predict behavioral lapses in this sustained-attention driving task.

5.3.3 EFFECTS OF AROUSING AUDITORY SIGNALS ON THE EEG

Next, this study explored temporal spectral dynamics preceding, during and following fatigue-related behavioral lapses and following arousing warning. Figure 5.3

shows time courses of spectral changes in the bilateral occipital area following ineffective warning (light blue trace), effective warning (red trace), and without warning (dark blue trace), compared to those of the alert trials (black trace). Figure 5.3 shows that both theta- an alpha-band power steadily increased prior to the lane-departure onset (at time 0 sec). Again, the trends of steady increasing theta- and alpha-band power leading to behavioral lapses in the three groups of drowsy trials were nearly identical, indicating the robustness of the theta and alpha augmentation preceding the behavioral lapses.

Figure 5.3 also shows that after the lane-departure onset (at time 0 sec), the alpha (top panel) and theta (bottom panel) power abruptly decreased by over 10 dB and 5 dB to nearly the alert (black trace) baseline, respectively. More importantly, following the subjects' responses, the spectra of trials with ineffective warning (light blue trace) and without warning (dark blue trace) rapidly rose from the alert baseline to the drowsy level in 5-15 sec. The theta and alpha power of trials with effective warning, however, remained low for ~40 sec. The green horizontal lines mark the time points when the difference between the spectra of trials with effective warning and without warning were statistically significant ($p<0.01$). The spectral difference between the trials with effective warning and without warning was significant from 7 to 18 sec in alpha band and from 7 to 21 sec in the theta band ($p<0.01$). Furthermore, the spectral difference between the trials with effective and ineffective warning was significant from 7 to 16 sec in both alpha and theta bands (brown horizontal lines).

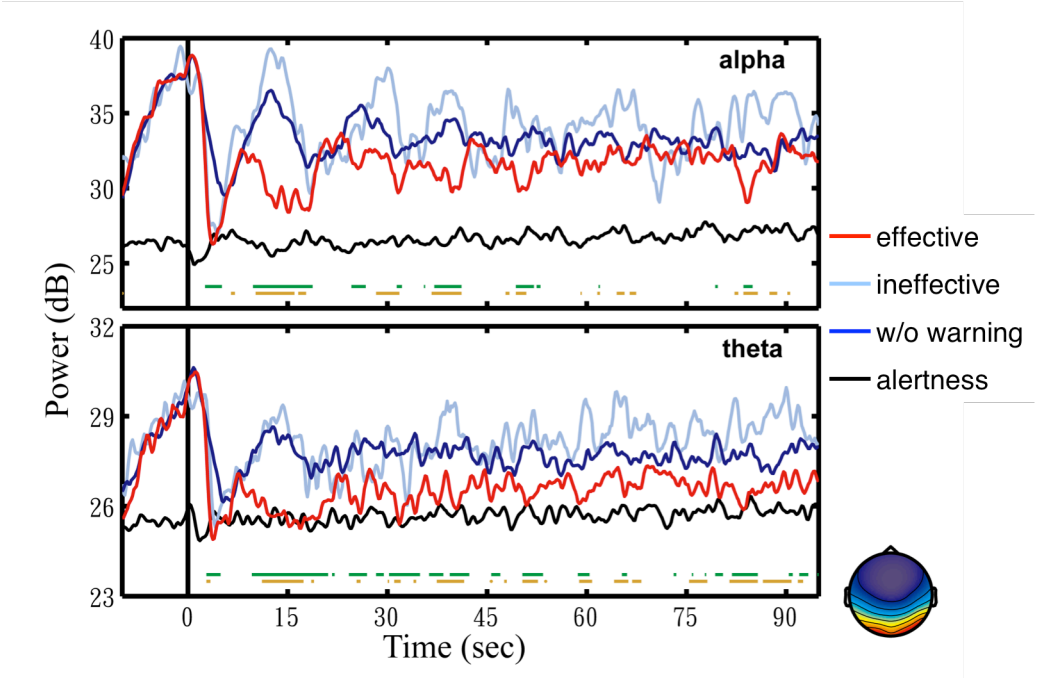

Figure 5.3 Average component EEG power changes in alpha (top panel) and theta (bottom panel) bands from the bilateral occipital components (lower right corner). All the trials are aligned to the lane-deviation onsets at time 0 sec (vertical solid black line). The red, light blue, dark blue, and black traces are the averaged spectra of trials with effective feedback, with ineffective feedback, without feedback, and in alertness, respectively. The green horizontal line indicates the statistically significant differences ($p< 0.01$) between trials with effective feedback and without feedback. The brown indicates the statistically significant differences ($p< 0.01$) between trials with effective feedback and ineffective feedback.

In sum, these results provided invaluable insights into the optimal electrode locations (lateral occipital region) and EEG features (theta- and alpha-band power) for a practical on-line closed-loop lapse detection and mitigation system detailed below. The EEG and behavioral data collected from this experiment were used to assess the EEG correlates of fatigue-related lapses and build a lapse prediction model for the second experiment.

5.4 DEVELOPING A OCLDM SYSTEM

Our previous study [77] proposed a smartphone based drowsiness monitoring and management system to continuously and wirelessly monitor brain dynamics using a lightweight, portable, and low-density EEG acquisition headgear. The system was designed to assess brain activities over the forehead, detect drowsiness, and deliver arousing warning to users experiencing momentary cognitive lapses, and assess the efficacy of the warning in near real-time. However, the system was not fully implemented nor experimentally validated in humans. Furthermore, according to the neurophysiological results in Section 3, EEG signals collected over the lateral occipital regions were more informative for lapse detection. This study extends the previous work to design, develop, and test an OCLDM System.

5.4.1 SYSTEM ARCHITECTURE

Figure 5.4(a) shows the system diagram of the proposed OCLDM System. The system consists of two major components: (1) a mobile platform featuring the OCLDM algorithm, and (2) a mobile and wireless 4-channel headgear measuring EEG signals over the hair-bearing occipital regions with dry EEG sensors [80]. The OCLDM System was implemented as an App on an Android-based platform (e.g. Samsung Galaxy S3). The smartphone has a Bluetooth module, 16GB RAM, an ARM Cortex-A9 processor, Android (Ice Cream Sandwich) OS, and other components. When the App is launched, it can automatically search and connect to a nearby EEG headgear to receive data from the EEG acquisition headgear. In the mean time, the

App opened an USB port to receive the events from a four-lane highway scene to synchronize the EEG data and scene events. The build-in speaker (or plug-in a ear set) of the smartphone delivers auditory warning signal once the OCLDM System detects that the subject is experiencing a cognitive lapse. Both the EEG data and scene-generated events could be logged onto either smartphone's build-in memory or an external microSD card for further analysis.

The mobile and wireless EEG acquisition headgear features a 4-channel lightweight portable bio-signal acquisition device powered by a 3.7v Li-ion battery [77]. It consists of a TI MSP430 microprocessor, a pre-amplifier, a battery-charging circuit, a 24bit ADC, a Bluetooth module, and dry spring-loaded EEG sensors [80]. The spring-loaded probes of the sensor can penetrate the hair to provide good electrical conductivity with the scalp. The microprocessor controls all the components including the amplifiers, digitizers, and transmits the digitalized EEG data to the Bluetooth module. The 4-channel EEG data are then transmitted to the authorized receiver of the OCLDM System. Depending on the applications, the system's sampling rate can be programmed at 128, 256, or 512 Hz. An experienced subject can easily put on this EEG acquisition device within 1-3 min without any help from a technician. Figure 5.4(b) shows a photo of a subject wearing a 4-channel EEG headgear and performing the simulated driving experiment.

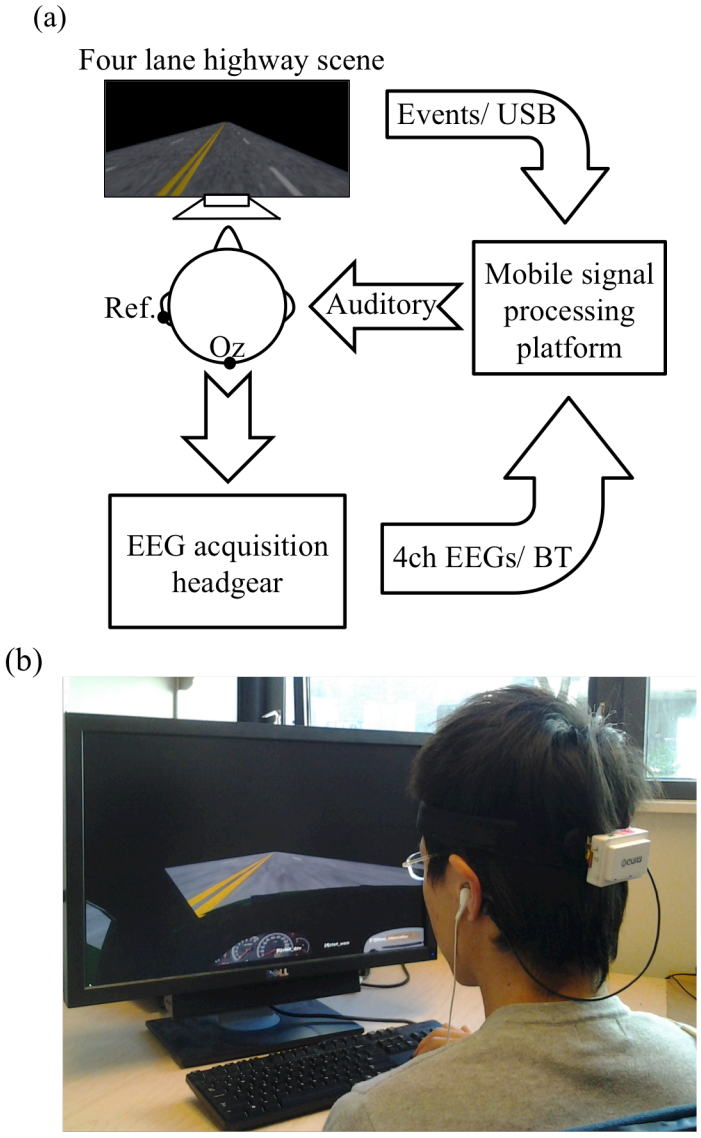

Figure 5.4 The system diagram of the proposed OCLDM System. (a) The EEG headgear collected 4-channel brain activities from the lateral occipital area while a subject was performing the lane-drifting experiment. The mobile signal-processing platform received the acquired EEG raw data through Bluetooth, and the event markers generated from the lane-departure scene through an USB interface. Finally, the auditory feedback was delivered to the subject when the averaged EEG power across four channels was 3dB over the alert baseline. (b) A photo of a subject performing the on-line driving experiment while wearing a 4-channel EEG headgear (the white small box attached on a flexible band) over the lateral occipital area.

5.4.2 SYSTEM SOFTWARE DESIGN

Figure 5.5 shows the program's state diagram of the proposed OCLDM System. Three major states, including Baseline Collecting (BC), Driving Performance Monitoring (DPM), and Warning Efficacy Assessment (WEA), were implemented in the program. When the program is launched, one can modify the parameters in the SETTING page, shown as a square box in the figure. For instance, the parameters can be the duration of baseline data collection, or the threshold of auditory warning delivering for the other two states. Depending on the applications, the lapse threshold in the DPM state can be calculated accordingly. For example, one can use a combination of power of alpha, beta, theta, and delta bands to detect cognitive lapse. The program then enters the next (DPM) state after the Baseline (calibration) data collection has completed. The DPM module continuously monitors the driver's neurophysiological data. The program stays in the DPM state until the lapse threshold is met, which depends on the neurophysiological results as shown in Section 5.3. For instance, when the subject's power spectrum in alpha band is 3dB higher than the threshold (alert baseline collected in the BC state), the program delivers an auditory warning to arouse the subject and enters the FEA state. The current value is stored as the lapse reference in the FEA module. The system repeatedly delivers auditory warning until the EEG power decreases to another threshold.

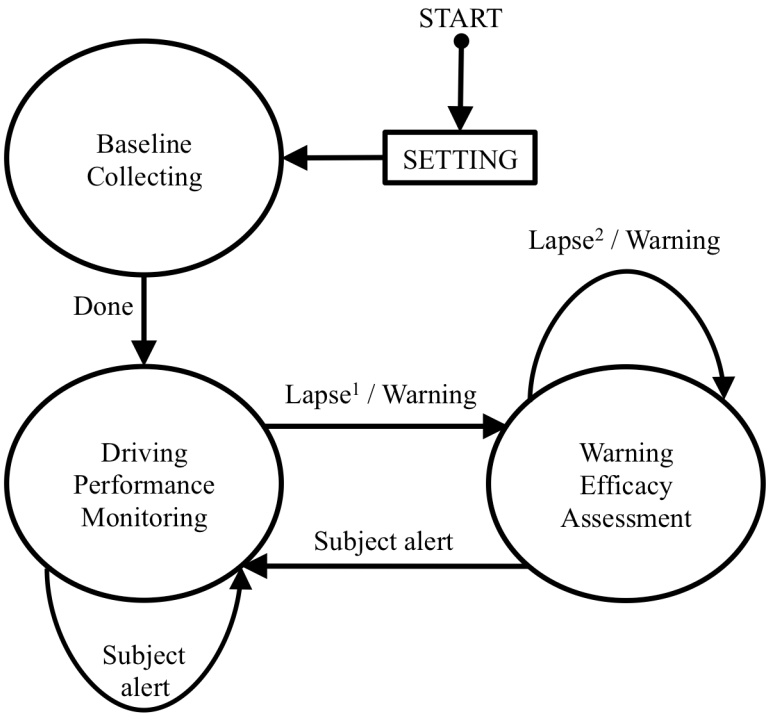

Figure 5.5 The software state diagram of the OCLDM System. The program first goes through SETTING and Baseline collecting state. Then, the system continuously detects and monitors subjects' driving performance until the EEG spectra indicate cognitive lapse. Note that, Lapse[1] represents the averaged EEG power across four channels is 3dB over the alert baseline. Lapse[2] represents that the averaged EEG power across four channels has not yet dropped 3dB from the lapse power.

5.4.3 ON-LINE EXPERIMENTAL PARADIGM

Three new male subjects (who did not participated in the first experiment) with normal hearing and aged 25-30 years old participated in the on-line closed-loop lane-departure driving experiments to evaluate the OCLDM System in a more naturalistic setting (in a regular office without any electromagnetic shielding). All of them were asked to read and sign the informed consent form before participating in the studies.

The entire experiment consisted of a 1 min training and a ~60 min driving periods. During the training session, subjects were asked to stay fully alert. The averaged alpha power collected in the BC session was used as an alert baseline to determine whether a subject is experiencing cognitive lapses in the driving task. The subject performed the lane-departure driving experiments following the protocol below:

(1) Subjects seated in an armchair and the driving scene was displayed on a 27" monitor, placed at ~60cm in front of the subject.
(2) Subjects used a keyboard to control a vehicle cruising on a high way, i.e. a left key turns the simulated car to the left while a right key turns to the right.
(3) Four electrodes were placed over the lateral occipital area to collect EEG data noninvasively. The data were transmitted to a smartphone for processing via Bluetooth.
(4) When the averaged power spectra in alpha band met a certain criterion, arousing auditory warning (~65dB 1,750Hz tone-burst) would be delivered in half of these lapse episodes through an ear set to the subjects. Note that, the subjects didn't know the warning before the experiments.
(5) The arousing tone-burst would be continuously delivered to the subjects until the averaged power spectra in the alpha band has dropped 3dB from the lapse power.

The cognitive lapses were detected when the subject's alpha-band power, calculated by a moving-averaged STFT with a 256-point sliding window advanced at

1 sec step running on the smartphone, was 3 dB over the alert baseline power [55][81] and Results in Section 3). This study used the alpha power fluctuations to monitor cognitive lapses because (1) a recent study showed that the alpha augmentation was sensitive to the transition from full alertness to mediate drowsiness, while the theta augmentation was more sensitive to the transition from mediate to deep drowsiness; (2) the empirical results of this study showed that the augmentation of alpha-band power changes was greater than that of the theta-band power (Figure 5.2). The system would repeatedly deliver auditory warning until the alpha-band power amplitude has dropped to 3dB below the power level when the cognitive lapse was identified.

5.4.4 RESULTS FROM THE OCLDM SYSTEM

The numbers of detected cognitive lapses varied across subjects. Table 5.1 lists the numbers of trials with effective, ineffective warning and without warning, respectively. Here, the way we defined the effective trials was based on the RT in response to the lane-departure event immediately following the arousing signal (CT+1 whose RT was shorter than two times aRT); while the ineffective trials had RT longer than three times aRT.

Figure 5.6 shows the boxplot of behavioral performance (RTs) of trials with effective trials (red), ineffective trials (light blue), and without warning (dark blue), compared to the averaged aRT (black) during the on-line experiments. The effective trials had RTs comparable to the averaged aRT (less than 1 sec) in both CT and CT+1.

Table 5.1 Number of trials collected from the on-line experiment.

Subject	With auditory warning		Without auditory warning
	Effective	Ineffective	
1	20	2	21
2	17	1	24
3	23	0	27

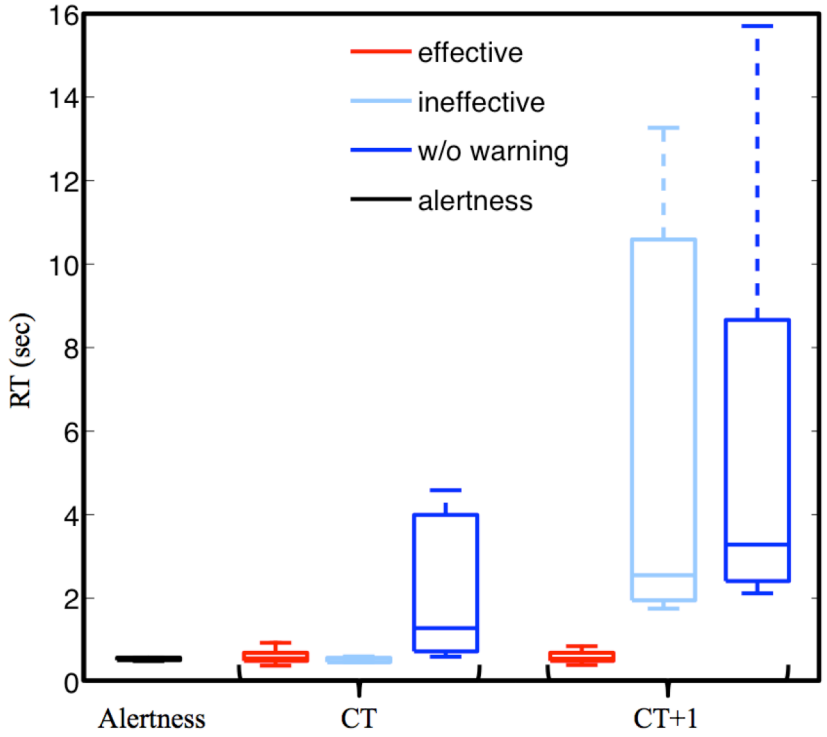

Figure 5.6 The behavioral performance comparison. Note that, the trials of with effective feedback (red), with ineffective feedback (light blue), and without feedback (blue), compared to alert trials (black) after removing the outliers.

Note that the RTs of CT+1 with effective versus ineffective warning differed largely because that was how the effective and ineffective trials were defined. However, the RTs of CT trials (red and light blue) of these two groups of trials were very comparable. That is, even though the subjects responded to the arousing warning by steering the simulated car immediately back to the cruising position, they could well be totally non-responsive to the very next lane-departure event. This finding is consistent to our off-line study reported in Section 3 in which the arousing warning was delivered to the subjects who just had a behavioral lapse.

Figure 5.7 showed the averaged alpha-band spectral time courses across subjects and trials with effective warning (red trace), with ineffective warning (light blue trace), and without warning (dark blue trace), compared to averaged aRT (black trace). All spectral time courses were aligned to the user response onset (thick vertical black line at time 0 sec), and the auditory warning for effective- and ineffective-trials were delivered ~5 sec before the user response. In the trials following effective auditory warning, the alpha power decreased steadily and reached the averaged aRT in ~7 sec. The power spectra remained as low as that of the alert baseline from 7 to 20 sec after response onset. In the trials with ineffective auditory warning, the spectral time series fluctuated fierously due to the small number of trials. In the trials without warning, the alpha power fluctuated before response onset and steadily dereased until ~7 sec. Thereafter, the alpha power increased again from ~7 sec to 13 sec, suggesting the subjects might be partially arouse by the lane-departure event and their own bebavioral reposense temportally but returned to the fatigue state rapidly thereafter.

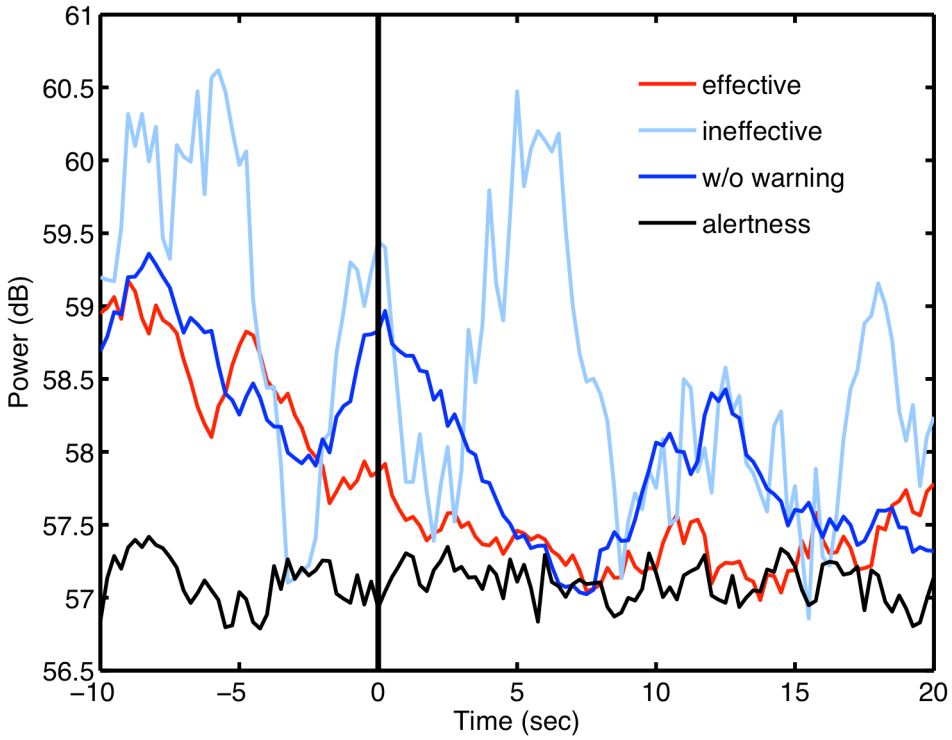

Figure 5.7 The averaged alpha power time course plotting time-locked to subject response onset (vertical solid line at time 0 sec). Averaged alpha power of trials with effective feedback (red trace), with ineffective feedback (light blue), and without feedback (blue trace), compared to trial with aRT (black). The time course of power was estimated by short time Fourier transform with 256 points of time window and 224 points overlapping.

5.5 CONCLUSION

Many studies have shown that the brain dynamics correlated with behavioral lapses can be assessed from EEG data. Recent studies have also shown auditory signals can arouse drowsy subjects and affect EEG activities [55][81]. However, in these studies, the arousing warning was delivered to subjects after they displayed behavioral lapses, which in reality may be too late because the behavioral lapse might

have already had catastrophic consequences. Therefore, a system that features real-time lapse detection and delivers warnings to the drowsy subjects is desirable in preventing catastrophic incidents while driving.

The first experiment of this study showed that EEG power changes in either alpha or theta band can be used as an indicator for assessing the subjects' fatigue (cf. Figure 5.3), and auditory warning temporarily reduces the alpha and theta band power and mitigates the behavioral lapses (cf. Figure 5.2(a)). In addition, EEG changes after delivery of auditory warning are a good indicator of the efficacy of arousing warning. More importantly and interestingly, empirical results of the first study showed that arousing auditory signals could always reliably mitigate human behavioral lapses, but these immediate behavioral responses could not guarantee the subjects were fully awake, alert, or attentive, similar to snooze after an alarm is turned off. This finding may open a new research direction of how to accurately confirm a subject's cognitive level for some sustained-attention tasks, such as an aircraft navigator or a long-haul truck driver. In other words, further studies to explore the brain changes in this sleep inertia period may provide valuable insights of brain dynamics during a transitional state of lowered arousal occurring immediately after awakening from sleep. Based on previous studies [55][81] and the results of the first experiment, this study further developed a truly on-line closed-loop lapse detection and mitigation system to detect/predict cognitive lapse based on the EEG spectra, deliver arousing warning on the occurrence of cognitive lapse, and assess the efficacy of the arousing warning, again, based on the EEG spectra. Most importantly, the EEG spectra changes within

~10 seconds after delivering arousing warning were closely monitored, such that any false-awake situations could be decreased. This study then documented the design, development, and on-line evaluation of the proposed OCLDM System that featured a lightweight wireless EEG acquisition headgear and a smartphone-based signal-processing platform. Experimental results showed that subjects' EEG power could almost remain at the alert state without bouncing back to the drowsy level (cf. Figure 5.7). These results suggest that the proposed system could prevent potential behavioral lapses based solely on the EEG signals, and this demonstration could lead to a real-life application of the dry and wireless EEG technology and smartphone-based signal-processing platform. An interesting question is if the neural correlates of fatigue could be generalized across different sustained-attention tasks and different recording conditions. In the past few years, we have conducted several sustained-attention tasks, including auditory target detection tasks [63], visual compensatory tracking tasks [76], and simulated driving tasks [19][82] and found that performance-related EEG dynamics were comparable across tasks [83]. Results of these studies also showed the fatigue-related brain dynamics were quite consistent across different recording environments (within a well-controlled EEG laboratory vs. a 6-degree-of-freedom motion platform) and responding methods (using a button press or a steering wheel). Therefore, it is reasonable to believe the methods developed under this study could be translated from laboratory settings to real-world environments.

In sum, this study demonstrated the feasibility of translating a laboratory-based passive BCI system to a neuroergonomic device that is capable of continuously

monitoring and mitigating operator neurocognitive fatigue using a pervasive smartphone in real-world environments. The passive BCI technologies might also be applicable to other real-world cognitive-state monitoring, such as attention, distraction, comprehension, confusion, and emotion. We thus believe more real-world passive BCI implementations will emerge in the foreseeable future.

ACKNOWLEDGEMENTS

This chapter contains material from "Developing an EEG-based On-line Closed-loop Lapse Detection and Mitigation System" by Yu-Te Wang, Kuan-Chih Hunag, Chun-Shu Wei, Teng-Yi Huang, Li-Wei Ko, Chin-Teng Lin, Chung-Kuan Cheng, and Tzyy-Ping Jung, which appears in the *Frontiers in Neuroscience*, 2014. The dissertation author was the first investigator and author of this paper.

Chapter 6

Conclusion and Future Works

BCI systems have been studied for more than two decades; however, moving this laboratory-based paradigm to real-life applications still suffers from many challenges. Moreover, easy-of-use without compromising reliability in home-based clinical applications also plays an important role in the real-world applications of BCI systems.

This study details the components of SSVEP-based BCI systems. From our perspective, three main concerns needed to be addressed to translate this system from a laboratory demonstration to a real-life application: (1) the lack of precise visual stimulus presentation on mobile platforms; (2) the difficulty of assessing SSVEPs from easily accessible locations; (3) the lack of a truly portable, user-acceptable (e.g. comfortable and wearable), and robust system for monitoring and processing EEG data from unconstrained users. For the first concern, this study proposed a frame-rate based approach to render visual stimuli. Given the empirical results, the mobile devices in the current market can indeed render accurate visual stimuli and to induce SSVEPs. To address concern 2, this study systematically and quantitatively compared SSVEPs from different scalp and face locations using high-density EEG data. The

comparison between hair-covered and non-hair-bearing areas showed that the quality of SNR depends on the electrodes selection. From the empirical results, the SNR of combinational channels can perform better than one channel measured on the occipital over visual cortex in less than 4 channels for some subjects. For concern 3, this thesis proposed a portable, wireless, low-cost EEG system and a smartphone-based signal-processing platform into a truly wearable online SSVEP-based BCI system.

With a modular design, the components of the above-mentioned BCI systems also can be applied to other applications, such as continuous fatigue monitoring (Chapter 5) or routine EEG data collection (Chapter 4). More precisely, the smartphone-based signal-processing platform discussed in Chapter 4 can also be programmed to realize other BCI applications. For example, the current system can be easily converted into a motor-imagery-based BCI through detecting spectral changes of mu/beta rhythms over the sensorimotor areas. In essence, Chapters 4 and 5 are just two sample demonstrations of the smartphone-based platform technology that can enable and/or facilitate numerous BCI applications in real-world environments. My future work involves exploring and testing more applications of wearable BCI systems.

BIBLIOGRAPHY

[1] J. R. Wolpaw, N. Birbaumer, D. J. McFarland, G. Pfurtscheller, and T. M. Vaughan, "Brain-computer interfaces for communication and control", *Clinical Neurophysiology*, vol. 113, pp. 767–791, 2002.

[2] J. R. Wolpaw and E. W. Wolpaw "Brain-Computer Interfaces: something new under the sun", in *Brain-Computer interfaces principles and practice* J. R. Wolpaw and E. W. Wolpaw (eds.), pp. 3-12, New York: Oxford, 2012.

[3] B. Z. Allison, S. Dunne, R. Leeb, J. D. R. Millan, and A. N.ijholt, "Recent and upcoming BCI progress: overview, analysis, and recommendations", in *Towards Practical Brain-Computer Interfaces, Bridging the Gap from Research to Real-World Applications*, B. Z. Allison, S. Dunne, R. Leeb, J. D. R. Millan, and A. N.ijholt (eds.) pp. 1-13, London: Springer, 2011.

[4] D. Regan, Human Brain Electrophysiology: Evoked Potentials and Evoked Magnetic Fields, in Social Science and Medicine, New York: *Elsevier*, 1989.

[5] Y. -T. Wang, Y. Wang, and T. -P. Jung, "A Cell-phone based Brain Computer Interface for Communication in Daily Life", *Journal of Neural Engineering*, vol. 8, no. 2, pp. 1-5, 2011.

[6] M. D. Tommaso, V. Sciruicchio, M. Guido, G. Sasanelli, and F. Puca, "Steady-state visual evoked potentials in headache: diagnostic value in migraine and tension-type headache patients", *Cephalalgia*, vol. 19, pp. 23-26, Jan. 1999.

[7] American Migraine Fundation [Online]. Avaliable: http://www.americanmigrainefoundation.org/about-migraine/

[8] Y. Wang, Y. -T. Wang, and T.-P. Jung, "Visual stimulus design for high-rate SSVEP BCI", *Electronics Letters*, vol.46, no. 15, pp. 1057-1058, 2010.

[9] Y. -T. Wang, Y. Wang, C. K. Cheng, T. -P. Jung, "Developing Stimulus Presentation on Mobile Devices for a Truly Portable SSVEP-based BCI", *in Proc. 35th Int. IEEE EMBS Conf.*, 2013.

[10] M. Cheng, X. Gao, S. Gao, and D. Xu, "Design and implementation of a brain–computer interface with high transfer rates," *IEEE Trans. on Biomed. Eng*. vol.10, pp. 1181-1186, October 2002.

[11] S.P. Kelly, E.C. Lalor, R.B. Reilly, J.J. Foxe, "Visual spatial attention tracking using high-density ssvep data for independent brain–computer communication," *IEEE Trans. on Neural Systems and Rehab. Eng.*, vol.13, pp. 172-178, 2005.

[12] X. Gao, D. Xu, M. Cheng and S. Gao, "A BCI-based environmental controller for the motion-disabled", *IEEE Trans. Neural Syst. Rehabil. Eng.* pp.137-140, 2003.

[13] K. -K. Shyu, P. -L. Lee, M. -H. Lee, M. -H Lin, R. -J. Lai and Y. J. Chiu, "Development of a Low-Cost FPGA-Based SSVEP BCI Multimedia Control System", *IEEE Trans. Biomed. Circuits and Systems*, vol. 4, pp. 125-132, 2010.

[14] G. Bin, X. Gao, Z. Yan, B. Hong, and S. Gao, "An online multi-channel SSVEP-based brain-computer interface using a canonical correlation analysis method", *Journal of Neural Engineering*, vol. 6, no. 4, 2009.

[15] C. -T. Lin, L. -D. Liao, Y. -H. Liu, I -J. Wang, B. -S. Lin, and J. -Y. Chang. , "Novel Dry Polymer Foam Electrodes for Ling-Term EEG Measurement", *IEEE Trans. on Biomed. Eng.,* vol. 58, pp. 1200-1207, May 2011.

[16] J. -C. Chiou, L. -W. Ko, C. -T. Lin, C. -T. Hong, T. -P. Jung, S. -F. Liang, and J. -L. Jeng, "Using novel mems eeg sensors in detecting drowsiness application", *in Biomedical Circuits and Systems Conference, 2006. BioCAS 2006. IEEE*, Nov. 2006, pp. 33 –36.

[17] C. Grozea, C. D. Voinescu, and S. Fazli, "Bristle-sensors Low-cost Flexible Passive Dry EEG Electrodes for Neurofeedback and BCI Applications", *Journal of Neural Engineering*, vol.8, no.2, pp. 1-5, 2011.

[18] Y. M. Chi, Y. -T. Wang, Y. Wang, C. Maier, T. -P. Jung, G. Cauwenberhs, "Dry and Don-contact EEG Sensors for Mobile Brain-Computer Interfaces", *IEEE Trans. on Neural Syst. And Rehab. Eng*. vol. 20, pp. 228-235, March 2012.

[19] C. -T. Lin, L. -W. Ko, J. -C. Chiou, J. -R. Duann, T. -W. Chiu, R. -S. Huang, S. -F. Liang, and T. -P. Jung, "A noninvasive neural prosthetic platform using mobile and wireless EEG", *Proc. IEEE,* vol. 96, no. 7, pp. 1167-1183, 2008.

[20] C. -T. Lin, Y. -C. Chen, T. -T. Chiu, L. -W. Ko, S. -F. Liang, H. -Y. Hsieh, S. -H. Hsu, and J. -R. Duan, "Development of Wireless Brain Computer Interface With Embedded Multitask Scheduling and its Application on Real-Time Driver's Drowsiness Detection and Warning", *IEEE Trans. Biomed. Eng.,* vol. 55, pp. 1582-1591, 2008.

[21] R. Schneiderman, "DSPs evolving in consumer electronics applications*", IEEE Signal Processing Mag.*, vol. 27 pp. 6-10, 2010.

[22] Y. Wang, X. Gao, B. Hong, and S. Gao, "Practical designs of brain computer interfaces based on the modulation of EEG rhythms", in B. Graimann, G. Pfurtscheller (Eds.) Invasive and Non-Invasive Brain-Computer Interfaces, *Springer*, The Frontiers Collection, 2010.

[23] M. Kaleb, C. –T. Lin, K. S. Oie, T. –P. Jung, S. Gordon, K. W. Whitaker, S. –Y. Liu, S. –W. Liu, and W. D. Hairston, "Real-World Neuroimaging Technologies," *Access, IEEE*, vol. 1, pp. 131-149, 2013.

[24] M. Cheng and S. Gao, "An EEG-based Cursor Control System", *IEEE BMES/EMBS conference*, vol. 1, 1999.

[25] Z. Wu, Y. Lai, Y. Xia, D. Wu, and D. Yao, "Stimulator selection in SSVEP-based bci", *Med. Eng. Phys.*, vol. 30, no. 8, pp. 1079-1088, 2008.

[26] G. Bin, X. Gao, Y. Wang, B. Hong, and S. Gao "VEP-Based Brain-Computer Interfaces: Time, Frequency, and Code Modulations", *IEEE Computational Intelligence Mag.,* pp. 22-26, 2009.

[27] M. Cheng , X. Gao, S. Gao and D. Xu, "Design and implementation of a brain-computer interface with high transfer rates", *IEEE Trans. Biomed. Eng.*, vol. 49, pp. 1181-1186, 2010.

[28] L. J. Trejo, R. Rosipal, and B. Matthews, ''Brain-computer interfaces for1-D and 2-D cursor control: Designs using volitional control of the EEG spectrum or steady-state visual evoked potentials,'' *IEEE Trans. Neural Syst. Rehab. Eng*., vol. 14, no. 2, pp. 225–229, 2006.

[29] S. P. Kelly, E. C. Lalor, C. Finucane, G. McDarby, and R. B. Reilly, ''Visual spatial attention control in an independent brain-computer interface,'' *IEEE Trans. Biomed. Eng*., vol. 52, no. 9, pp. 1588–1596, 2005.

[30] Y. Wang, R. Wang, X. Gao, B. Hong, and S. Gao, "A practical VEP-based brain–computer interface", *IEEE Trans. Neural Syst. Rehabil. Eng*., vol. 14, no. 2, pp. 234–239, 2006.

[31] I. Sugiarto, B. Allison, and A. Graser, "Optimization strategy for SSVEP-based BCI in spelling program application", *ICCET'08. Int. Conf. on Computer Engineering and Technology*, vol. 1, pp. 223–226, 2009.

[32] Y. Wang, R. Wang, X. Gao, and S. Gao, "Brain-computer interface based on the high-frequency steady-state visual evoked potential", *Proceeding of IEEE Neural Interface and Control,* pp. 37-39, 2005.

[33] G. Edlinger and C. Guger, "Can dry EEG sensors imporve the usablity of SMR, P300 and SSVEP based BCIs?", in Towards Practical Brain-Computer Interfaces, Bridging the Gap from Research to Real-World Applications, B. Z. Allison, S. Dunne, R. Leeb, J. D. R. Millan, and A. N.ijholt (eds.) pp. 281-300, London: *Springer*, 2011.

[34] EmotivSystems. Emotiv - brain computer interface technology [Online]. Available: http://emotiv.com.

[35] g.tec Medical Engineering [Online]. Available: http://www.gtec.at.

[36] R. Srinivasan, "Acquiring brain signals from outside the brain", in Brain-Computer interfaces principles and practice J. R. Wolpaw and E. W. Wolpaw (eds.), pp. 105-122, New York: *Oxford*, 2012.

[37] E., Donchin and M. G. H., Coles, "Is the P300 component a manifestation of context updating", *Behavioral and Brain Sciences*, vol. 11, no. 3, pp. 357-374, 1988.

[38] D. J. Krusienske, D. J. McFarland, and J. C. Principe, "BCI signal processing: feature extraction", in Brain-Computer interfaces principles and practice J. R. Wolpaw and E. W. Wolpaw (eds.), pp. 123-145, New York: *Oxford*, 2012.

[39] F. Lotte, M. Congedo, A. Lecuyer, F. Lamarche, and B. Arnaldi, "A review of classification alrorithms for EEG-based brain-computer interfaces", *J. Neural Eng.*, vol.4, 2007.

[40] A. J. Bell and T. J. Sejnowski, "An Information-Maximization Approach to Blind Separation and Blind Deconvolution," *Neural Computation*, vol. 7, pp. 1129-1159, 1995.

[41] S. Makeig, T.-P. Jung, A. J. Bell, D. Ghahremani, and T. J. Sejnowski, "Blind separation of auditory event-related brain responses into independent components," *Proceedings of the National Academy of Sciences*, vol. 94, pp. 10979-10984, September 30, 1997 1997.

[42] A. Hyvarinen, E. Oja, "Independent component analysis: algorithms and aapplication", *Neural Netw*., vol.13, pp. 411-430, 2000.

[43] T. W. Lee, M. Firolami, and T. J. Sejnowski, "Independent component analysis using an extended infomax algorithm for mixed subgaussian and supergaussina sources", *Jeural Computation*, vol 11, pp. 417-441, 1999.

[44] J. N. Knight, "Signal Fraction Analysis and Artifact Removal in EEG", PhD thesis in Colorado State University, 2003.

[45] C. -T. Lin, L. -W. Ko, M. -H. Chang, J. -R. Duann, J. -Y. Chen, T. -P. Su and T. -P. Jung, "Review of wireless and wearable Electroencephalogram systems and brain-computer interfaces - a mini-review", *Gerontology*, vol. 56, pp. 112-119, 2010.

[46] Y. Wang, X. Gao, B. Hong, C. Jia, and S. Gao, "Brain–computer interfaces based on visual evoked potentials - feasibility of practical system designs*", IEEE Eng. Med. Biol. Mag*., vol. 17, no. 5, pp. 64-71, 2008.

[47] H. D. Croo, M. Bandmann, G. M. Mackay, K. Rumar, and P. V. Vollenhoven, "The Role of Driver Fatigue in Commercial Road Transport Crashes", *European Transport Safety Council*, 2001.

[48] National Sleep Foundation, Summary findings of the 2005 sleep in America poll. Arlington, VA, USA, 2005

[49] National Highway Traffic Safety Administration. Drowsy driving and automobile crashes. eds. *N.H.T.S. Administration*. New Jersey, USA.

[50] The Royal Society for the Prevention of Accidents. Driver fatigue and road accidents. A literature review and position paper. Edgbaston, Birmingham, UK. 2001.

[51] L. M. Bergasa, J. Nuevo, M. A. Sotelo, R. Barea, and M. E. Lopez, "Real-time system for monitoring driver vigilance," *IEEE Trans. On Intelligent Transportation Systems*, vol. 7, pp. 63-77, 2006.

[52] T. D'Orazio, M. Leo, C. Guaragnella, and A. Distante, "A visual approach for driver inattention detection," *Pattern Recognition*, vol. 40, pp. 2341-2355, 2007.

[53] M. Golz, D. Sommer, U. Trutschel, B. Sirois, and D. Edwards, "Evaluation of fatigue monitoring technologies," *Somnologie - Schlafforschung und Schlafmedizin*, vol. 14, pp. 187-199, 2010.

[54] C. -T. Lin, T. -Y. Huang, W. -C. Liang, T. -T. Chiu, C. -P. Chao, S. -H. Hsu, and L. -W. Ko, "Assessing effectiveness of various auditory warning signals in maintaining drivers' attention in virtual reality-based driving envirionments", *Perceptual and Motor Skills*, vol. 108, pp. 825-835, 2009.

[55] C. –T. Lin, K. –C. Huang, C. -F. Chao, C. –H., Chuang, L. –W., Ko, and T. –P. Jung, "Can Arousing feedback rectify Lapses in driving? Prediction from EEG power spectra. *J. Neural Eng.* Vol.10, 2013

[56] T. Zander, C. Kothe, S. Jatzev, and M. Gaertner, "Enhancing Human-Computer Interaction with Input from Active and Passive Brain-Computer Interfaces," in Brain-Computer Interfaces, D. S. Tan and A. Nijholt, Eds., ed: *Springer London*, pp. 181-199, 2010.

[57] T. O. Zander and S. Jatzev, "Context-aware brain–computer interfaces: exploring the information space of user, technical system and environment," *Journal of Neural Engineering*, vol. 9, p. 016003, 2012.

[58] T. O. Zander, C. Kothe, S. Welke, and M. Roetting, "Utilizing Secondary Input from Passive Brain-Computer Interfaces for Enhancing Human-Machine Interaction," in Foundations of Augmented Cognition. Neuroergonomics and Operational Neuroscience. vol. 5638, D. Schmorrow, et al., Eds., ed: *Springer Berlin Heidelberg*, pp. 759-771. 2009.

[59] M. Lehne, K. Ihme, A. M. Brouwer, J. van Erp, and T. O. Zander, "Error-related EEG patterns during tactile human-machine interaction," in *Affective Computing and Intelligent Interaction and Workshops*, pp. 1-9, 2009.

[60] Y. Dong, Z. Hu, K. Uchimura, and N. Murayama, "Driver inattention monitoring system for intelligent vehicles: A review", in *IEEE Intelligent Vehicles Symposium*, pp. 875-880, 2009.

[61] S. Makeig and M. Inlow," Lapses in alertness: coherence of fluctuations in performance and EEG spectrum", *Electroencephalography and Clinical Neurophysiology*. Vol.86, pp. 23–35. 1993.

[62] T. Kecklund and T. Akerstedt, " Sleepiness in long-distance truck driving: an ambulatory EEG study of night driving", Ergonomics vol. 36, pp. 1007–1017. 1993.

[63] T. –P. Jung and S. Makeig, " Prediction failures in auditory detection from changes in the EEG spectrum", in *proceeding of the 17th Annual International Conference of the IEEE Engineering in Medicine and Biology Society*, pp. 927–928, 1995.

[64] P. R. Davidson, R. D. Jones, M. Peiris, and T. R. Davidson, " EEG-based lapse detection with high temporal resolution*", IEEE Trans. Biomed. Eng.* Vol. 54, pp. 832–839, 2007.

[65] J. A. Horne and S. D. Baulk, "Awareness of sleepiness when driving," *Psychophysiology*, vol. 41, pp. 161-165, 2004.

[66] H. Eichele, H. Juvodden, M. Ullsperger, and T. Eichele, "Maladaptation of event-related EEG responses preceding performance errors," *Frontiers in Human Neuroscience*, vol. 4, 2010-August-10 2010.

[67] T. Eichele, S. Debener, V. D. Calhoun, K. Specht, A. K. Engel, K. Hugdahl, D. Y. von Cramon, and M. Ullsperger, "Prediction of human errors by maladaptive changes in event-related brain networks," *Proceedings of the National Academy of Sciences*, vol. 105, pp. 6173-6178, April 22, 2008 2008.

[68] S. Debener, M. Ullsperger, M. Siegel, K. Fiehler, D. Y. von Cramon, and A. K. Engel, "Trial-by-Trial Coupling of Concurrent Electroencephalogram and Functional Magnetic Resonance Imaging Identifies the Dynamics of Performance Monitoring," *Journal of Neuroscience*, vol. 25, pp. 11730-11737, 2005.

[69] B. T. Jap, S. Lal, and P. Fischer, "Comparing combinations of EEG activity in train drivers during monotonous driving," *Expert Systems with Applications*, vol. 38, pp. 996-1003, 2011.

[70] M. Simon, E. A. Schmidt, W. E. Kincses, M. Fritzsche, A. Bruns, C. Aufmuth, M. Bogdan, W. Rosenstiel, and M. Schrauf, "EEG alpha spindle measures as indicators of driver fatigue under real traffic conditions," *Clinical Neurophysiology*, vol. 122, pp. 1168-1178, 2011.

[71] R. Rosipal, B. Peters, G. Kecklund, T. Åkerstedt, G. Gruber, M. Woertz, P. Anderer, and G. Dorffner, "EEG-Based Drivers' Drowsiness Monitoring Using a Hierarchical Gaussian Mixture Model," in Foundations of Augmented Cognition. vol. 4565, D. Schmorrow and L. Reeves, Eds., ed: *Springer Berlin Heidelberg*, 2007, pp. 294-303.

[72] T. A. Dingus, D. V. McGehee, N. Manakkal, S. K. Jahns, C. Carney, C., and J. M. Hankey, "Human factors field evaluation of automotive headway maintenance/collision warning devices", *Human Factors,* vol. 39, pp. 216–229, 1997.

[73] C. Spence and J. Driver, "Inhibition of return following an auditory cue The role of central reorienting events," *Experimental Brain Research*, vol. 118, pp. 352-360, 1998/01/01 1998.

[74] Y. -C. Liu, "Comparative study of the effects of auditory, visual and multimodality displays on drivers' performance in advanced traveller information systems," *Ergonomics*, vol. 44, pp. 425-442, 2001.

[75] C. Ho, H. Z. Tan, and C. Spence, "Using spatial vibrotactile cues to direct visual attention in driving scenes," *Transportation Research Part F: Traffic Psychology and Behaviour*, vol. 8, pp. 397-412, 2005.

[76] T. –P. Jung, K. –C. Huang, J. –A. Cheng, L. –W. Ko, T. –W Chai, C. –T. Lin, "Arousing feedback rectifies lapse in performance and corresponding EEG power spectrum," in *IEEE 2010 Annual International Conference*, pp. 1792-1795, 2010.

[77] Y. –T. Wang, C. –K. Huang, C. –T. Lin, Y. Wang, and T. –P. Jung, "Cell-phone based Drowsiness Monitoring and Management system," *in IEEE Biomedical Circuits and Systems Conference (BioCAS)*, pp. 200-203, 2012.

[78] A. Delorme and S. Makeig, "EEGLAB: an open source toolbox for analysis of single-trial EEG dynamics including independent component analysis*," Journal of Neuroscience Methods*, vol. 134, pp. 9-21, 2004.

[79] T.-P. Jung, S. Makeig, M. Westerfield, J. Townsend, E. Courchesne, and T. J. Sejnowski, "Analysis and visualization of single-trial event-related potentials," *Human Brain Mapping*, vol. 14, pp. 166-185, 2001.

[80] L. –D. Liao, I. –J. Wang, S. –F. Chen, J. –Y. Chang, and C. –T. Lin, “Design, fabrication and experimental validation of a novel dry-contact sensor for measuring electroencephalography signals without skin preparation”, *Sensors* Vol. 11, pp. 5819-5834, 2011.

[81] C.-T. Lin, K.-C. Huang, C.-F. Chao, J.-A. Chen, T.-W. Chiu, L.-W. Ko, and T.-P. Jung, "Tonic and phasic EEG and behavioral changes induced by arousing feedback," *NeuroImage*, vol. 52, pp. 633-642, 2010.

[82] C. -T. Lin, R. -C. Wu, S.-F. Liang, T. -Y. Huang. W. -H Chao, Y.-J. Chen, T. -P. Jung, “EEG-based Drowsiness Estimation for Safety Driving Using Independent Component Analysis”, *IEEE Transactions on Circuit and System*, vol. 52, pp. 2726-2238, 2005.

[83] R. -S. Huang, T. -P. Jung, and S. Makeig, “Event-related brain dynamics in continuous sustained-attention tasks, ” in Foundations of Augmented Cognition, eds. D. Schmorrow and L. Reeves. (*Springer Berlin Heidelberg*), pp. 65–74, 2007